TITLE: Final Report: Thermopile Energy Harvesting for Subsurface Wellbore Sensors

AUTHORS: Charles Bryan, Thomas Dewers, Jason Heath, Ramesh Koripella, Jiann-Cherng Su, and Aaron Melad

Final Report
Submitted January 23, 2023

Project FWP number: FWP-20-022728
Period of performance: October 1, 2020 - December 15, 2022

SUBMITTED BY
Sandia National Laboratories
1515 Eubank Blvd. SE
Albuquerque, NM 87123
DUNS: 0071132280000

SUBMITTED TO
U.S. Department of Energy
National Energy Technology Laboratory

PRINCIPAL INVESTIGATOR
Charles Bryan
(505) 980-8641
crbryan@sandia.gov

X 

Charles R. Bryan

Signed by: CHARLES BRYAN (Affiliate)

Issued by Sandia National Laboratories, operated for the United States Department of Energy by National Technology & Engineering Solutions of Sandia, LLC. SAND2023-xxxx.

Sandia National Laboratories is a multimission laboratory managed and operated by National Technology and Engineering Solutions of Sandia, LLC, a wholly owned subsidiary of Honeywell International, Inc., for the U.S. Department of Energy's National Nuclear Security Administration under contract DE-NA0003525.

Final Report: Thermopile Energy Harvesting for Subsurface Wellbore Sensors

Charles Bryan, Thomas Dewers, Jason Heath, Ramesh Koripella, Jiann-cherng Su, and Aaron Melad
Sandia National Laboratories

Abstract

Robust *in situ* power harvesting underlies all efforts to enable downhole autonomous sensors for real-time and long-term monitoring of CO_2 plume movement and permeance, wellbore health, and induced seismicity. This project evaluated the potential use of downhole thermopile arrays, known as thermoelectric generators (TEGs), as power sources to charge sensors for *in situ* real-time, long-term data capture and transmission. Real-time downhole monitoring will enable "Big Data" techniques and machine learning, using massive amounts of continuous data from embedded sensors, to quantify short- and long-term stability and safety of enhanced oil recovery and/or commercial-scale geologic CO_2 storage.

This project evaluated possible placement of the TEGs at two different wellbore locations: on the outside of the casing; or on the production tubing. TEGs convert heat flux to electrical power, and in the borehole environment, would convert heat flux into or out of the borehole into power for downhole sensors. Such heat flux would be driven by pumping of cold or hot fluids into the borehole—for instance, injecting supercritical CO_2—creating a thermal pulse that could power the downhole sensors. Hence, wireless power generation could be accomplished with *in situ* TEG energy harvesting.

This final report summarizes the project's efforts that accomplished the creation of a fully operational thermopile field unit, including selection of materials, laboratory benchtop experiments and thermal-hydrologic modeling for design and optimization of the field-scale power generation test unit. Finally, the report describes the field unit that has been built and presents results of performance and survivability testing. The performance and survivability testing evaluated the following: 1) downhole power generation in response to a thermal gradient produced by pumping a heated fluid down a borehole and through the field unit; and 2) component survivability and operation at elevated temperature and pressure conditions representative of field conditions. The performance and survivability testing show that TEG arrays are viable for generating ample energy to power downhole sensors, although it is important to note that developing or connecting to sensors was beyond the scope of this project. This project's accomplishments thus traversed from a low Technical Readiness Level (TRL) on fundamental concepts of the application and modeling to TRL-5 via testing of the fully integrated field unit for power generation in relevant environments. A fully issued United States Patent covers the wellbore power harvesting technology and applications developed by this project.

Acknowledgments

The U.S. Department of Energy's (DOE) National Energy Technology Laboratory (NETL) funded this research under project number FWP-20-022728. The authors thank Andrew Knight for many technical reviews over the course of the project and George El-kaseeh of the New Mexico Institute of Mining and Technology and the Southwest Regional Partnership on Carbon Sequestration for helpful discussions and information on wellbore and tubing sizes and operations at an active enhanced oil recovery and CO_2 storage site. Adam Foris, formerly of Sandia National Laboratories, developed initial designs of the small-scale benchtop power harvester prototype for this project.

CONTENTS

LIST OF FIGURES

LIST OF TABLES

ACRONYMS AND DEFINITIONS

Abbreviation	Definition
API	American Petroleum Institute
EPA	Environmental Protection Agency
EPDM	ethylene propylene diene monomer
EOR	enhanced oil recovery
FTDI	Future Technology Devices International [data port]
FWU	Farnsworth Unit
ID	inner diameter
NETL	National Energy Technology Laboratory
NMT	New Mexico Institute of Mining and Technology
OD	outer diameter
PCB	power conditioning board
$scCO_2$	supercritical CO_2
SNL	Sandia National Laboratories
SWP	Southwest Regional Partnership on Carbon Sequestration
TE	thermoelectric
TEG	thermoelectric generator
USDW	underground source of drinking water

1. Introduction

Robust *in situ* power harvesting underlies all efforts to enable downhole autonomous sensors for real-time and long-term monitoring of CO_2 plume movement and permeance, wellbore health, and induced seismicity. The objective of this project was to evaluate the potential use of downhole thermopile arrays, known as thermoelectric generators (TEGs) as power sources to charge sensors for *in situ* real-time, long-term data capture and transmission. Real-time downhole monitoring will enable "Big Data" techniques and machine learning, using massive amounts of continuous data from embedded sensors, to quantify short- and long-term stability and safety of enhanced oil recovery and/or commercial-scale CO_2 storage.

In this project, we evaluated possible placement of the TEGs at two different wellbore locations, on the outside of the casing, or on the production tubing. TEGs convert heat flux to electrical power, and the concept developed and tested in this project is that, in the borehole environment, TEGs could convert heat flux into or out of the borehole into power for downhole sensors. Such heat flux would be driven by pumping of fluids into or out of the borehole—for instance, injecting supercritical CO_2—creating a thermal pulse that could power the downhole sensors. Hence, wireless power generation could be accomplished with *in situ* TEG energy harvesting.

This project final report provides a summary of the thermopile project. It provides background and summarizes the work done for the project, including selection of materials (Section 2), and laboratory benchtop experiments and thermal-hydrologic modeling carried out to design and optimize a field-scale power generation test unit (Section 3). The report describes the design and construction of a prototype field unit and presents results of performance and survivability testing (Sections 4 and 5). The performance and survivability testing evaluated the following: 1) downhole power generation in response to a thermal gradient produced by pumping a heated fluid down a borehole; and 2) survivability and operation at elevated temperatures and pressures relevant to downhole conditions. The tests were successful in demonstrating that downhole power generation using TEG arrays is a feasible approach for generating ample power for downhole sensors. Finally, the report concludes with lessons learned, recommendations for future work, and conclusions (Sections 6 and 7) with a focus on connecting TEGs to sensors to support testing and monitoring goals of commercial-scale geologic CO_2 storage, including real-time and long-term monitoring of external mechanical integrity.

1.1. Background

Subsurface storage of supercritical CO_2 ($scCO_2$) is the only feasible mechanism for sequestration of sufficient volumes of CO_2 to mitigate industrial production that greenhouse gas and its effects on climate change. However, the effects and potential risks of sequestering larger volumes of $scCO_2$ in subsurface reservoirs are poorly understood. Plume evolution, chemo-mechanical changes in wellbore, reservoir, or caprock properties, potential induced seismicity, and the development of possible leakage pathways are all of concern (Xia et al., 2017; Rhino et al., 2021; Simmons et al., 2022). In order to fully evaluate the possible risks and to demonstrate the long-term safety of subsurface CO_2 sequestration, continuous evaluation of reservoir conditions, caprock integrity, and borehole health conditions will be required by the Environmental Protection Agency (EPA) during the injection phase and during the post-injection monitoring phase (EPA, 2013). Wireline tools or permanently emplaced tools require power and data transmission via cables from the surface and cannot be deployed during normal borehole pumping or injection operations for injection or production wells. Also, wireline or permanently emplaced tools can only monitor conditions outside

the borehole in a limited way. For these reasons, the National Energy Technology Laboratory (NETL) has identified the development of downhole autonomous sensors for real-time and long-term monitoring of CO_2 plume movement and permeance, wellbore health, and induced seismicity as a high priority goal (DOE, 2017, 2020; NETL, 2021). Such sensors could be placed in the borehole, casing cement, and potentially the surrounding rock, are in development by other funded NETL projects (see the following for a list of active and past projects: https://netl.doe.gov/carbon-management/carbon-storage). An additional need for the sensors is a method for data transfer from the sensor to equipment within the borehole and from the sensor borehole depth to the surface. Finally, the autonomous sensors and data transmission equipment require a power source. Ideally, the power source is wireless, harvesting and storing power from the borehole environment and supplying it to the sensors in a controlled manner.

Power harvesting from the borehole environment is the focus of this study; other NETL-funded projects are evaluating sensor development and data transfer. Specifically, we evaluate the use of thermopiles, emplaced as arrays (thermoelectric generators, or TGEs) within the borehole, to generate electrical power at depth.

1.2. Thermopiles and TEGs

A thermocouple consists of a junction between two dissimilar metals, which generates a voltage as a function of temperature. If two thermocouples that are at different temperatures are connected, then the difference in voltage at each junction causes a current to flow between them. This is known as the Seebeck effect and is the principle behind thermopiles, which directly convert heat flux into electric power. Since a single pair of junctions generates only a very small current, many thermopiles are commonly connected together to form a thermoelectric generator (TEG). A TEG consists of P-type and N-type thermoelectric legs connected in series or series-parallel combination and sealed within robust upper and lower plates. Several TEGs can also be connected to increase the produced voltage or current. When a temperature differential (ΔT) is maintained between the upper and lower plates, a voltage is generated, and current can be drawn by connecting a load. Although efficiencies are low, TEGs are ideally suited for energy-harvesting applications, as they are solid-state with no moving parts; they are robustly built and very reliable in long-life applications. An example of a typical commercially available TEG is shown in Figure 1-1.

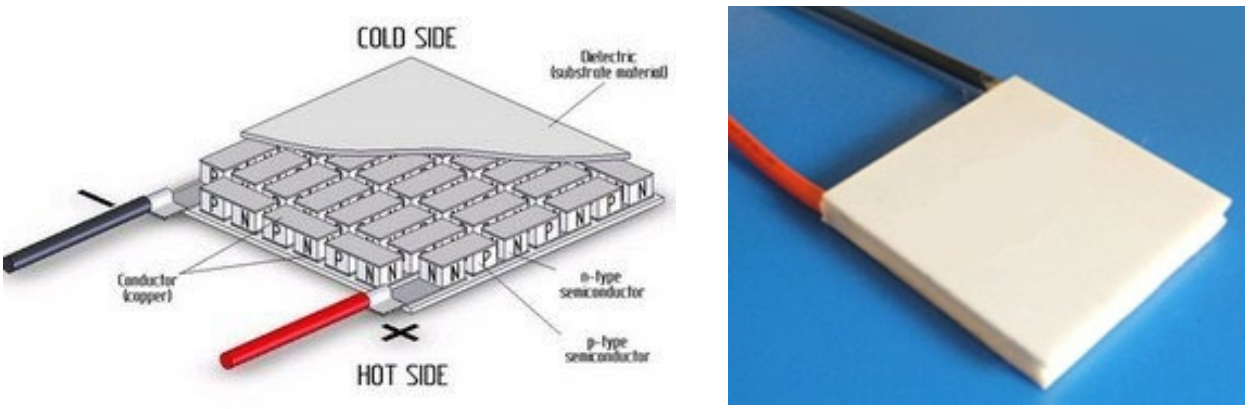

Figure 1-1. The design of a commercially available TEG. A series of P-type and N-type thermoelectric legs are connected in series or series-parallel to generate power from heat flux between the upper and lower plates.

The open circuit voltage of a TEG can be described by:

$$V_{oc} = S_{p-n} \times \Delta T \times N \quad \text{Eq. 1}$$

where S_{p-n} is the Seebeck coefficient of the P-N thermoelectric (TE) couple; ΔT is the temperature differential across the TE couple; and N is the number of TE couples in the module. Power (P) output depends on the load, so load optimization is required to achieve maximum power output. Depending on the resistive load, for maximum power, $V_{load} \sim \frac{1}{2} V_{oc}$. For a given TEG, V is proportional to ΔT, and P is proportional to ΔT^2.

For the proposed application, power is generated by periodic injections of hot or cold fluid; the voltage and power will vary as the ΔT first increases, and then decays after the pulse is stopped. Since the power output generated by the TEG energy harvesting method is not constant, directly powering the sensors, which will probably require a constant voltage input, is difficult. The solution for this is to store the energy generated by the TEGs in a battery and then provide a conditioned voltage input to the sensors. However, to safely operate (charge and discharge) the battery, conditioning of the TEG power output itself is required. The is accomplished with power management circuitry, which can also be used to provide sensors with a conditioned voltage input. Optimization of the number and wiring of the TEGs to produce voltage and current within effective operating range of the power conditioning circuitry is also required.

Hence, the energy harvesting system consists of the TEG modules that generate the electricity, the circuitry required to condition the TEG output for charging the battery, and a battery to store power. Moreover, the system must be designed to withstand the high temperatures and pressures that will be present in a $scCO_2$ injection or monitoring well.

1.3. Field Application of a TEG-Based Energy Harvesting System

TEGs convert heat flux to electrical power, and in the borehole environment, would be necessary to create a thermal gradient in order to generate power. This could be accomplished by pumping hot or cold fluids into the borehole, creating a transient thermal pulse and a heat flux to or from the borehole. By lining the casing or tubing with TEGs, this heat flux can be converted to electricity.

In the original proposal for this project, it was envisioned that the TEGs could be placed as a shell or sheath around the casing or tubing (Figure 1-2). However, as the project evolved, it became clear that a better approach would be to replace an entire section of casing or tubing with the power harvesting tool, which consists of a hollow shell with the TEGs sandwiched between the inner and outer walls. Such a configuration would be suited to injection wells such as EPA Class VI wells or for enhanced oil recovery (EOR) wells that undergo active injection and use tubing. The function of the casing or tubing strings would not be impacted by the replaced section; however, placement of the power harvesting unit in either the casing or the tubing string has many implications. If placed in the string casing string (Figure 1-2A), the unit could directly power co-located sensors, which could monitor conditions outside of the casing. It could provide power to any type of sensor, and the sensors could be located at critical locations such as the wall-rock/cement interface or the cement/casing interface. However, the unit would have to be emplaced when the borehole was drilled and cased; hence, this configuration could only be used for new boreholes and could be part of new wells being drilled for monitoring or as Class VI injection wells. Placing TEGs on the tubing (Figure 1-2B) would only provide direct power for sensors within the borehole. It could potentially support through-casing sensing of temperature profiles, thermal conductivity, resistivity, and potentially seismic/acoustic signals. However, this configuration offers the benefit that it could be done long after the borehole is drilled, although pulling and replacing tubing and packers is not

without technical risk or cost. As EPA Class VI requirements involve during- and post-injection monitoring via various wireline logging or other techniques for external mechanical integrity (i.e., flow behind casing), plume monitoring or other processes (EPA, 2013), the pulling of tubing will probably be common for injection wells. Although the general principle of the power harvester would allow it to be placed in either the casing or the tubing string, opportunities for placing the tool in an existing borehole, as part of the tubing string, are much more common. Hence for this project, the focus was on development of a tool for the emplacement on the tubing string.

The creation of thermal transients could be done purposefully to generate power or could be incidental to normal well operations—for instance, pumping of $scCO_2$ into an injection well at a CO_2 storage or enhanced oil recovery (EOR) site. However, a monitoring borehole could also be used if it were designed to allow cold fluids to be pumped down the tubing and up the annulus; the fluid would heat up as it flowed deeper into the well and back up the annulus to the power harvesting unit, creating a thermal gradient between the fluid in the tubing and in the annulus. In both cases, wireless electrical power generation for sensors or data transmission could be accomplished with *in situ* TEG energy harvesting. Note that an intermittent thermal pulse is necessary, as with constant pumping, a steady state thermal gradient with a very low ΔT would eventually be reached. Similarly, with no pumping, heat loss up the borehole would be insignificant, again producing too low a ΔT to generate power.

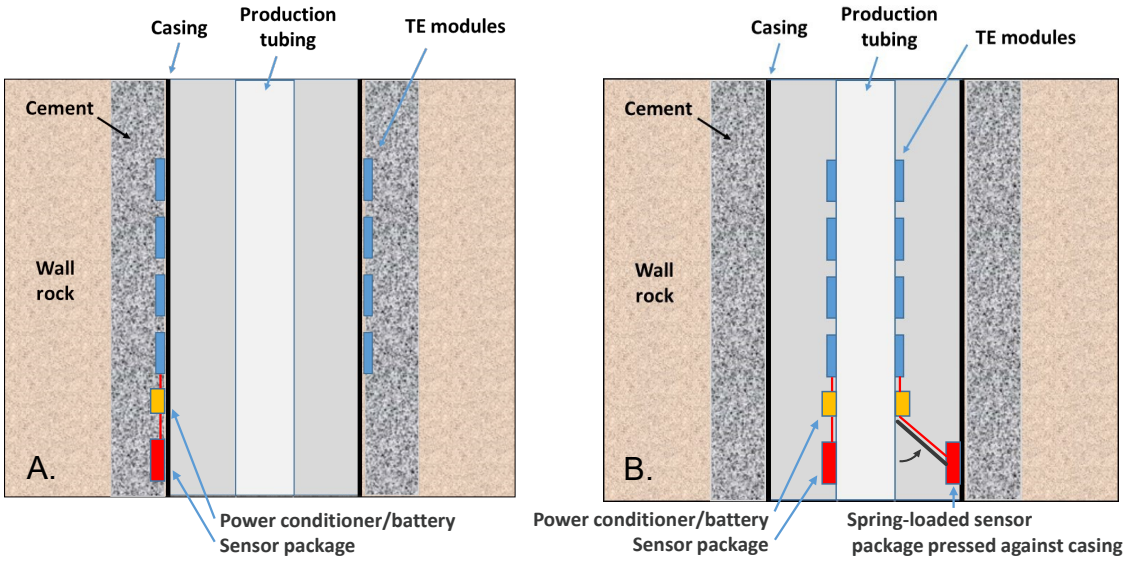

Figure 1-2. Two possible configurations for the TEG energy harvesting tool. A) TEGS placed on the casing, potentially powering sensors outside of the casing. B) TEGs placed on the tubing string, potentially directly powering sensors within the borehole.

The TEGs could be emplaced at any depth within the borehole, or even at several depths, to provide power for monitoring plume evolution, borehole health (e.g., CO_2 leakage through the casing cement), or other parameters within the reservoir, caprock, or overlying underground sources of drinking (USDWs). The EPA Class VI requirements in particular focus on protection of USDWs, and thus strategic placement of the TEGs could provide for monitoring of the caprock and locations upward to the USDWs. Wellbore integrity logging (e.g., cement-bond logs, etc.) in

new or existing wells could help identify locations where long-term monitoring would be helpful for TEG placement with appropriate sensors.

1.3.1. TEG power harvesting

In order to evaluate the types of thermal gradients and power generation that might be produced in a realistic CO_2 injection scenario, a spatio-temporal well-bore and surrounding country rock thermal and flow model was used to estimate temperature gradients experienced by TEGs secured and thermally coupled to production tubing. The model geometry is shown in Figure 1-3, using a 2-D axisymmetric set-up, axially aligned with the center of production tubing (shown in orange). The thermopile array is depicted in red in Figure 1-3A; moving radially from the center outward are depicted domains of production tubing, wellbore interior (green), wellbore casing (grey), cement (blue), and country rock (brown). The model itself solves partial differential equations of heat flow for the entire domain and Stokes flow through the production tubing via a fully coupled PARDISO solver using the COMSOL Multiphysics® software package. Thermal properties of the production fluid, cement, tubing, casing, and country rock are based on actual properties culled from the literature. An example of model output is shown in Figure 1-3B, which demonstrates temperature distributions in a wellbore experiencing transient flow of a cooling fluid.

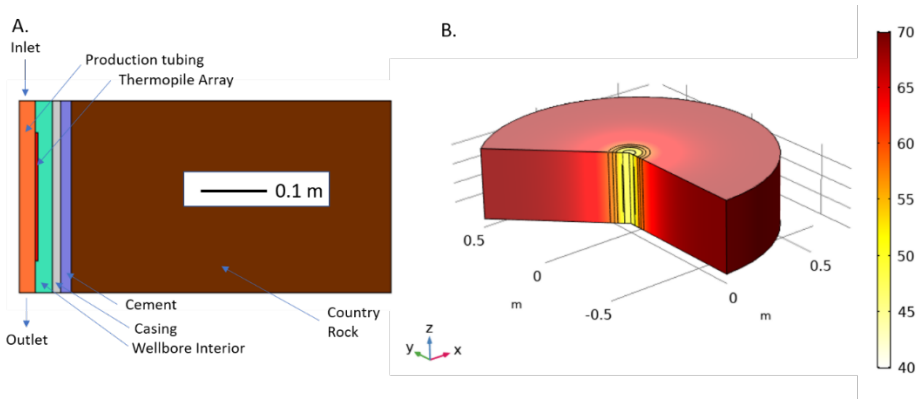

Figure 1-3. Geometry of wellbore mock-up in an axisymmetric geometry centered axially on the center of the production tubing. Moving outward from the left is the production tubing (orange), the thermopile array (red), the annulus between the production tubing and the casing (green), the wellbore casing (grey), cement (blue), and country rock (brown). B. Temperatures (°C) in the wellbore model arising from injection of cold fluid (50ºC) into the borehole, where the country rock and wellbore were existing at a steady temperature of 70°C.

Using the model described above, the temperature gradient experienced by the thermopile array, caused by a transient thermal pulse from fluid flow through the production tubing, can be calculated. For demonstration purposes, we assume a gaussian-shaped thermal pulse produced by pumping cold (40ºC) $scCO_2$ into a reservoir unit initially at thermal equilibrium with temperature of 70°C (343.15 K). The initial conditions and the reservoir rock properties are modeled after conditions at the Southwest Regional Partnership on Carbon Sequestration (SWP) Farnsworth Unit site, a site initially considered for the final field test of the power harvesting unit. This simulation assumed TEG arrays covered the production tubing and had a $S_{p\text{-}n}$ of 400 μV/K. The simulation extends to 48 hours, and the pulse extends over approximately 20 hours. The resulting evolution of temperature, ΔT, and the voltage produced by the TEGs is shown in
Figure 1-4. The reservoir is initially at 70ºC, cools near the wellbore, and then returns to the far-

field T. Integrated across the extent of the thermal pulse, the resulting power generation could be used to charge a downhole battery or power small sensors for immediate use.

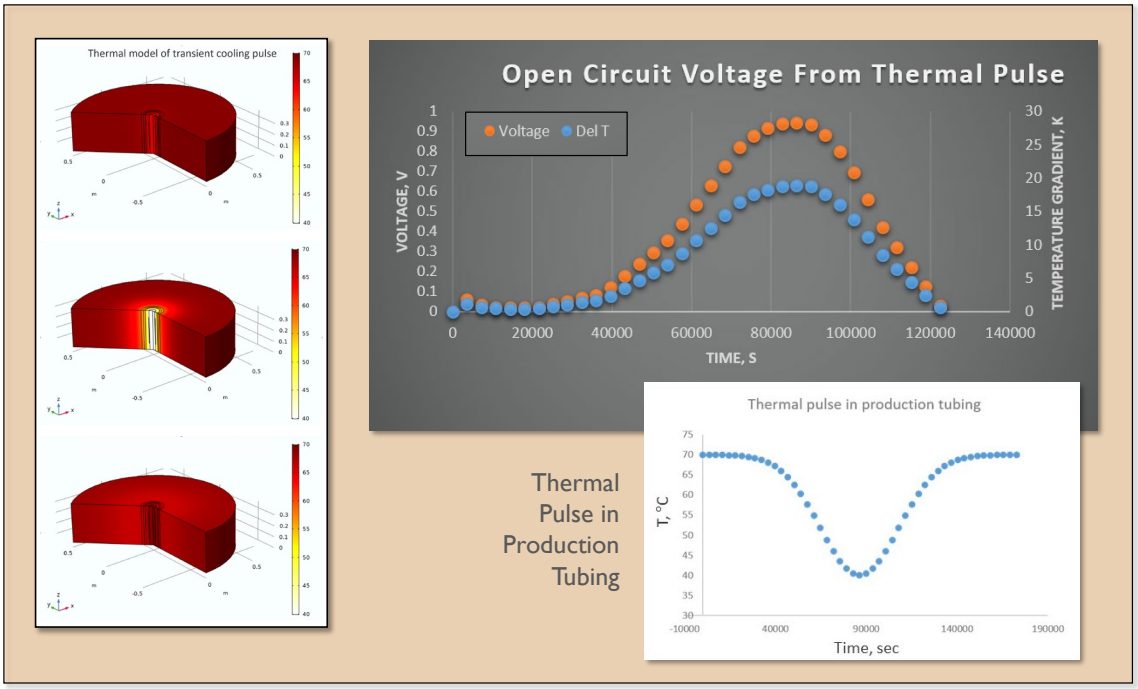

Figure 1-4. COMSOL model of thermal pulse and the resulting evolution of ΔT and TEG voltage.

1.3.2. Thermopile arrays as subsurface sensors

Under some conditions, an in-borehole TEG power harvesting unit may itself be used as a sensor to monitor conditions in the casing cement or in the surrounding wall rock. Supercritical CO_2 has an order-of-magnitude lower thermal conductivity than brines, and saturation of a porous reservoir rock by CO_2 could be expected to lower bulk thermal conductivities from roughly ~2 W/m-K to ~ 0.15 W/m-K as CO_2 saturation is increased from 0 to 1 (assuming a harmonic mean volumetric averaging; Hurter et al., 2007). Because the reservoir rock thermal conductivity will have a significant effect on the heat flux into the borehole, power generation by in-borehole TEGs may be used to sense changes in wall rock saturation.

Using the COMSOL model described above, a preliminary exploration into the ability of thermopile arrays to serve as sensors for the near-wellbore saturation of CO_2, has been carried out. For demonstration purposes, a gaussian-shaped thermal pulse of 50°C was assumed, passing through a wellbore system initially at thermal equilibrium with temperature of 50°C (343.15 K). The simulation extended to 48 hours, and the pulse extended over approximately 20 hours. The resulting temperature history at the inlet of the production tubing is shown by the red curve in Figure 1-5. The temperature gradient experienced across the thermopile array is shown by a series of curves for different wall rock thermal conductivities (shown by the legend in the figure) ranging from 0.75 to 3.0 W/m-K. This range is similar to that discussed by Hurter et al. (2007) for moving from brine-saturated to CO_2-saturated reservoirs. The variability in modeled temperature gradients suggests that measurable differences in temperature gradients and resulting open circuit voltages,

perhaps in the 10s of mVs, would occur with similar thermal pulse events across the saturation range investigated. This suggests that thermopile arrays on production tubing could be used to sense changes in saturation in nearby country rock. There may be similar sensing functions that could be used to measure Joule-Thompson cooling associated with leaking CO_2 within the cemented annulus.

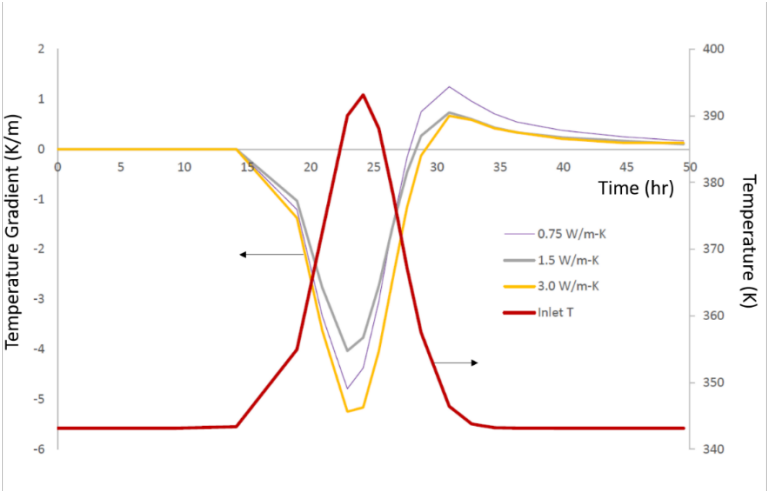

Figure 1-5. Gaussian-shaped thermal pulse, shown by the red curve, as experienced at the inlet of the simulated production tubing. The resulting temperature gradient experienced across the thermopile array is shown by a series of curves for different thermal conductivities of the country rock ranging from 0.75 to 3.0 W/m-K.

As described in the following sections, individual components were selected and tested to verify function over the temperature range of interest. Then, a small prototype of the energy harvesting system fabricated and used for benchtop testing and troubleshooting. Finally, a full-scale field prototype was built and tested at high pressure, high temperature conditions. At several stages during the project, COMSOL modeling was used, both to verify expected results and to help design the system and the planned field tests—for instance, for a given number of TEG modules, to determine the expected power generation for a given thermal pulse and ΔT in the field test. The project successfully met its goal of demonstrating the feasibility of the TEG energy harvesting approach for borehole applications.

2. Power generation system

The power generation system has three components, the TEGs, the power conditioning board (PCB), and the battery. As described below, the TEGs and battery are commercial off-the-shelf products, while the PCB was designed and built as SNL. Each was tested individually to determine performance at elevated temperatures, and then the system was assembled and benchtop tests were used to verify function and compatibility.

2.1. TEGS—selection and characteristics

Commercial TEGs were identified and procured for evaluation. The TEG used is a Marlow® TG12-2.5, a BiTe-based unit with dimensions of 1.18" × 1.34" × 0.159" thick, with rigid alumina ceramic plates on the top and bottom. This size is sufficiently small for 4-5 TEG modules to be placed radially around the tubing to generate power. The Seebeck coefficient ($S_{p\text{-}n}$) for this TEG is 400 μV/K. The specifications for this TEG indicate it is appropriate for continuous use up to 200°C. As the TEGs will be sandwiched between the inner assembly and the outer shell of the power harvesting unit, they will remain dry, and will not experience elevated pressures under field conditions. Typical power generation efficiencies for the Marlow TG12-2.5 are provided in Table 2-1. The Marlow® TEG is shown in Figure 2-1.

Table 2-1. TEG power generation as a function of ΔT

ΔT (K)	V_{oc} (V)	P (mW)
100	5.38	836.42
10	0.54	9.93
1	0.054	0.11

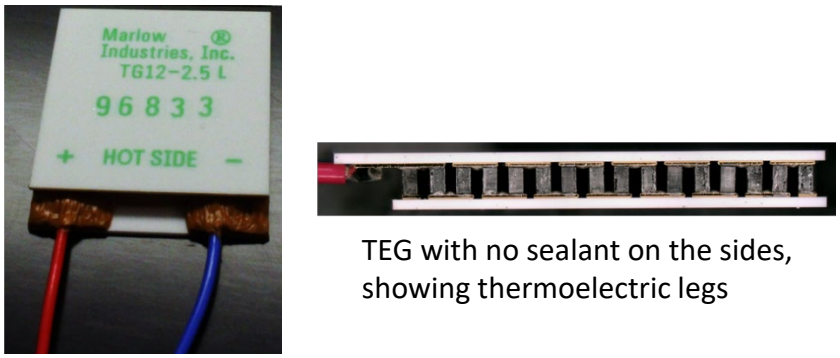

Figure 2-1. TEGs procured for the thermopile power harvesting tool.

Once received, laboratory ΔT tests were performed on the TEG to compare power generation with the vendor data sheet. In these tests, the TEG was sandwiched between a heat sink and a heating element (Figure 2-2), allowing development of a constant ΔT across the TEG module. The module performed as expected. Tests show that with a ΔT of approximately 5ºC, the expected power output is 2mW @0.4V. With a ΔT of 25ºC, the expected power output would be 30mW @0.4V. Over the range of expected ΔT values, it will be necessary to combine several TEGs in series to increase the voltage output to charge a battery or power a sensor.

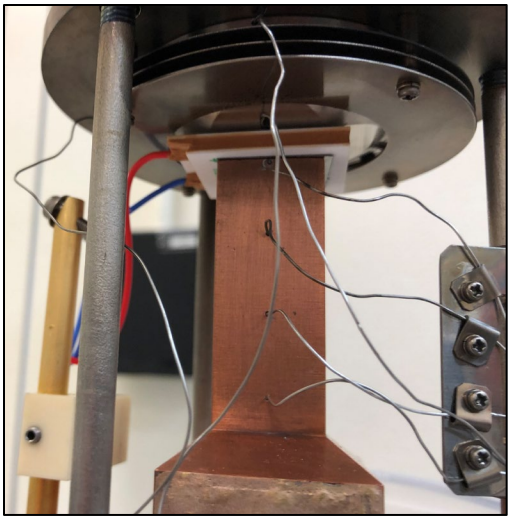

Figure 2-2. Experimental setup for verifying TEG performance.

In a second test, a TEG was bolted onto a steel cylinder using machined mounts that conformed to the cylinder surface to maximize heat transfer, and then a finned heat sink was attached to the top of the TEG (Figure 2-3). Heated air was flowed continuously through the pipe, generating a thermal pulse; the resulting ΔT was measured by thermocouples placed above and below the module. The goal of this test was to measure the TEG performance under less controlled conditions, potentially more realistic of the downhole environment. The experiment also provided a data set for initial COMSOL modeling of TEG performance.

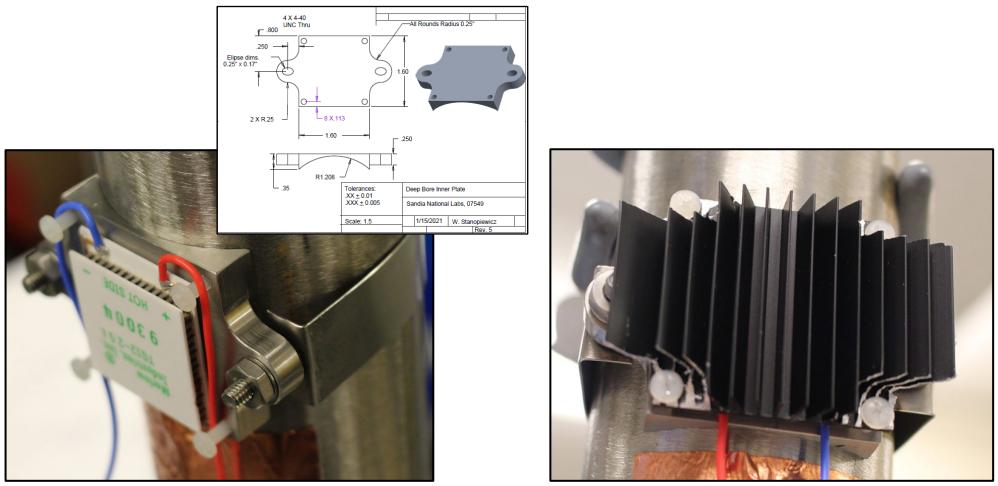

Figure 2-3. Testing of TEGs with mounts and heat sinks assembled around a cylinder to simulate borehole tubing or casing.

A COMSOL Multiphysics® model was developed for the test system shown in Figure 2-3. A wire-frame schematic of the system is shown in Figure 2-4. Also shown is a map showing the temperature distribution in the system during simulation of an actual TEG efficiency test. Measured data are compared with COMSOL model predictions in Figure 2-5. The measured and modeled results agree well, indicating that in a well-described system, COMSOL has the capabilities to accurately model TEG power production. It is notable, however, that the measured and modeled

results differed from the ideal efficiencies described by Marlow. This illustrates the need to accurately define the component geometries and thermal properties, and possibly even far-field boundary conditions, when predicting TEG power generation.

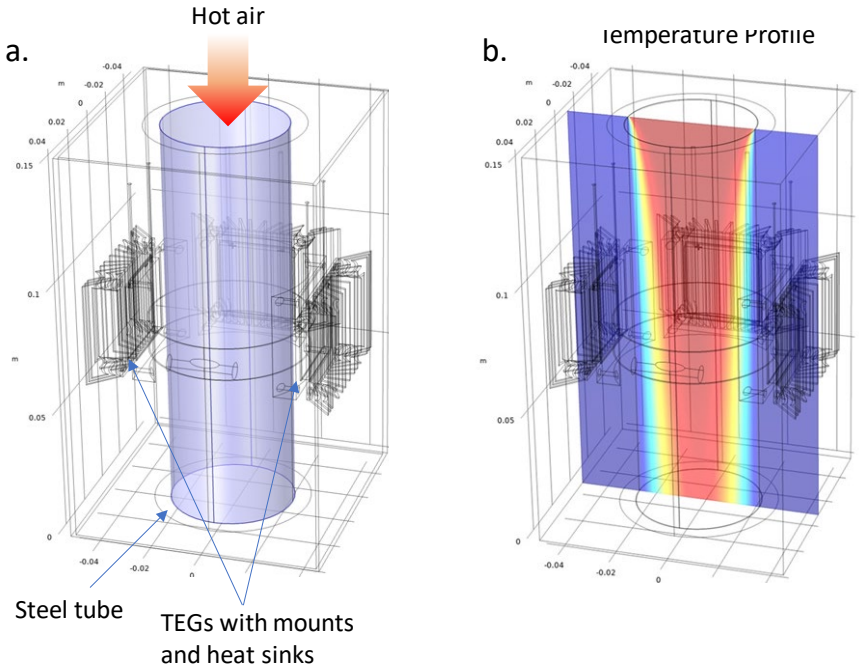

Figure 2-4. COMSOL model of ambient pressure test system. a) Wire-frame model of test system in COMSOL. b.) Thermal map resulting from simulation of an actual benchtop TEG efficiency test.

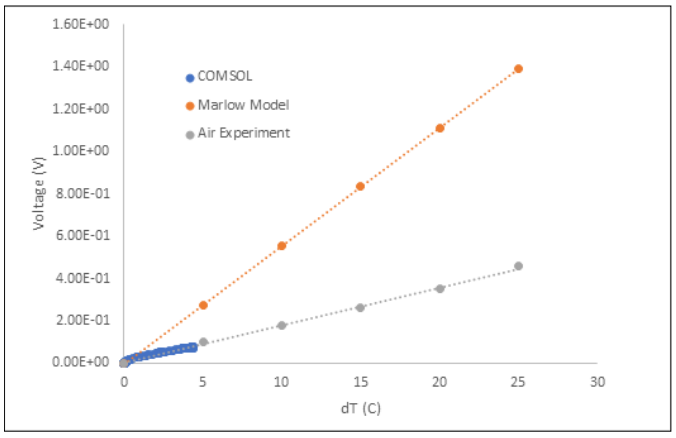

Figure 2-5. Comparison of measured test results and COMSOL model predictions of TEG power generation in the ambient-pressure test setup. Data and model results correspond well.

2.2. Power conditioning board

As noted in Section 1.2, the TEG output (voltage or power output) depends on the temperature differential across the TEG. Under energy harvesting conditions, the temperature differentials are expected to fluctuate, and thus the TEG output also fluctuates. A power conditioning circuit is needed to boost the output to the required voltage to charge a battery or to power a sensor. A commercial power conditioning evaluation board made by e-Peas, that will work with TEGs, was procured and tested under both ambient and high temperature (100°C) conditions (Figure 2-6). The e-Peas power conditioning board (green colored board) takes TEG output as low as 1.5V and boosts it to 3.5V for Li battery charging. In addition, it can also supply a regulated voltage output between 1.8-3.3V for sensor power. Laboratory tests showed that this power conditioning circuitry is satisfactory for the intended use, and it was repackaged onto a custom-build circuit board for downhole use (this work was done by the SNL Systems Research Department). The initial version of the PCB is shown in Figure 2-7, both as a schematic and as the final, populated card. This first-generation PCB included the power conditioning circuitry and connections for the TEG array and a board-mounted coin battery; it took the TEG voltage and boosted it to charge a battery. However, the board did not have a microcontroller, so could not record how much power has generated or how much energy was stored in the battery. These parameters had to be monitored with external electronics wired to the PCB.

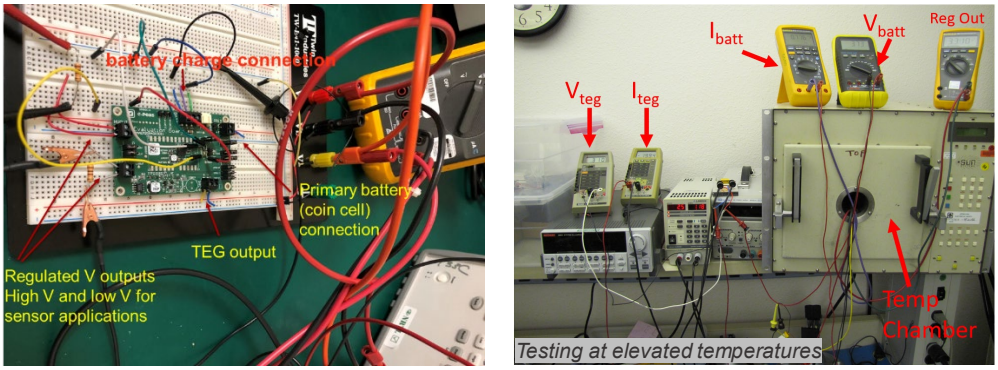

Figure 2-6. E-Peas power conditioning board under benchtop evaluation.

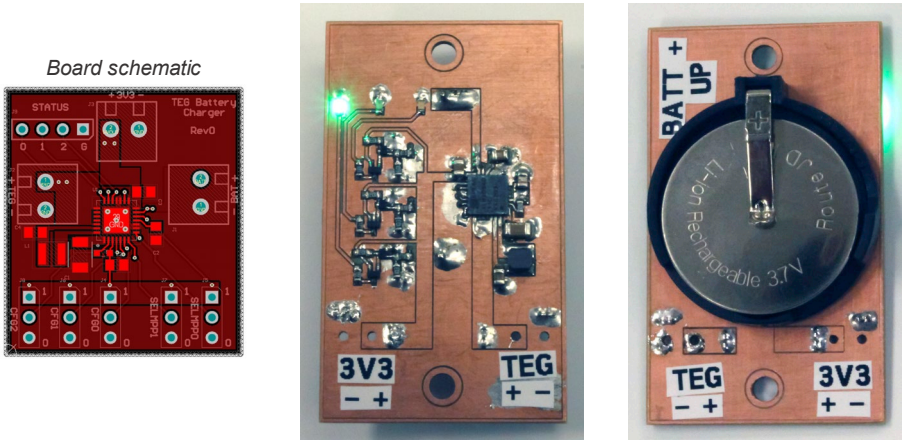

Figure 2-7. Schematic and printed version of the preliminary PCB card.

The Version 1 PCB was used in testing the laboratory prototype of the power harvester, as hard wiring the board to monitor TEG and battery performance was possible. However, for testing of the field prototype, the PCB had to be redesigned to independently monitor and store data tracking TEG and battery performance. To do this, a microcontroller and memory were incorporated into Version 2 of the PCB (Figure 2-8) for data management and memory for data storage. The board was also redesigned to include ports for three thermistors, a Future Technology Devices International (FTDI) data port, and connectors for the larger off-board battery used in the power harvesting unit field test. These additions allowed the power management system to monitor temperatures at different locations within the power harvester, and to monitor the operation of the TEG array and the battery during the field test. To facilitate counting of total power harvested even if the battery was full, a method to discharge the battery briefly to make it available for charging again while keeping track of total charge collection was also incorporated.

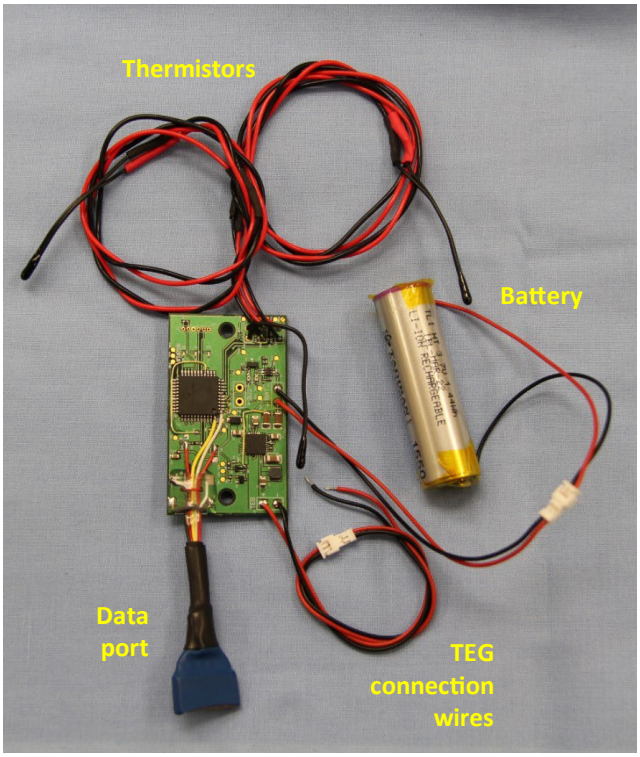

Figure 2-8. Version 2 of the PCB featured an added microprocessor and added memory for data management and storage, and three thermistors for monitoring temperatures within the power harvesting unit.

All electronic components on the PCB were laboratory tested to operate at temperatures of 80ºC. The initial of the Version 2 PCB failed at temperatures above about 60ºC, exhibiting an unacceptably high sleep current. After some debugging, the high current drain was traced to a micro-USB connector on the board and it was replaced in the in the final iteration with the FTDI port. The improvements in the Version 2 PCB will allow it to accurately monitor power harvesting and storage during the field test. Also, in an actual field deployment, the addition of the microcontroller and memory for data management could potentially allow the power harvesting unit to act as a data accumulation and storage center for downhole sensors.

2.3. Battery

For laboratory testing of the Version 1 PCB with the TEGs, a standard Li-ion coin cell was used. Finding a rechargeable battery to operate at temperatures of 70ºC or higher proved to be a challenge. Standard Li-ion rechargeable batteries have a maximum temperature for charging operations of 45ºC, and a maximum temperature for discharging operations of 60ºC. While high temperature rechargeable batteries are available for borehole use, their physical dimensions are too large to be used in our power harvester. Initially, we identified a small capacity Seiko coin battery (MS920T) that can operate up to 85°C, retaining up to 90% capacity after 85ºC exposure for 100 days. However, the battery capacity is low, only 6.5 mAh, requiring that 9 such batteries be connected in parallel for the field prototype, for a total capacity of 58 mAh.

However, within the last 6 months of the project, a more effective rechargeable high temperature Li-ion battery became available. The battery is 4.0 V Tadiran Lithium Ion Battery, Model TLI-1550HT. It is AA-sized, with dimensions just small enough to fit within the power harvester. It has an operating range for charging and discharging of -40º to 135ºC, with a nominal capacity of 500 mAh. It has a much higher capacity than the Seiko coin cell, or even several coin batteries linked in series. Laboratory testing of the Tadiran batteries showed that they were effective for our application, and they were incorporated into the field prototype.

3. Building and testing the benchtop prototype

Although testing individual components was necessary to confirm function, building a fully functional benchtop prototype was necessary for several reasons. First, testing at simulated field conditions must be carried out to aid in system design for the fielded system. The benchtop prototype was used to measure performance of the TEGS emplaced within the power harvesting tool, and to optimize the system geometry to maximize power production. Second, data from the benchtop prototype, collected under carefully controlled conditions, was used to calibrate and validate the COMSOL model for power generation under field conditions. Third, the high pressure benchtop prototype was built for robustness and survivability testing to verify component operation at downhole pressures and temperatures., Finally, the other major goal for the laboratory testing was to determine the energy production efficiency of the unit, information necessary to determine how may TEGs are required for the PCB electronics on the field prototype to function properly. Given estimates of the heat flux through the wall of the field prototype, this information was used to determine required number of TEGs and the necessary size of the field prototype.

Because electronics and TEGs are relatively fragile and must not be wetted, the basic design for the power harvester is a hollow sleeve, with the TEGS, battery, and PCB sandwiched in-between the inner and outer shells. (Figure 3-1). The inner and outer shells are sufficiently robust to withstand the pressures that are anticipated to occur in a CO2 injection borehole, protecting the electronics within. O-rings seal the unit, maintaining dryness in the cavity between the shells; the O-rings are ethylene propylene diene monomer (EPDM) rubber, a material frequently used for $scCO_2$ applications, as it resists CO_2-related degradation to which other O-ring materials, such as Viton, are susceptible. For field use, the package is intended to be placed between tubing sections in the tubing string, such that the inner wall of the sleeve is part of the tubing string. The actual length of the sleeve would depend upon how many TEGS are required to produce the desired power.

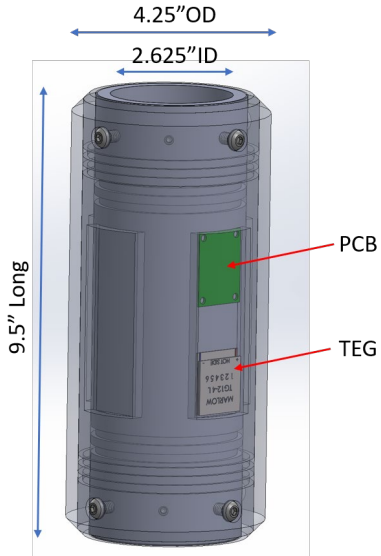

Figure 3-1. Schematic of high pressure/high temperature system for testing TEG power generation at downhole conditions.

For laboratory testing, the laboratory prototype was modified to fit the constraints of the laboratory test system, which has a smaller diameter than anticipated field boreholes. The major components of the system are visible in Figure 3-2. The prototype holds up to four TEGs, which are held

against the inner housing. A cap or thermal bridge covers each TEG, and is bolted to the inner housing, holding the TEG in place. The thermal bridges are intended to maintain good thermal contact between the TEGs and the outer shell, directing heat flow through the TEGs. A single Version 1 PCB, with an attached coin cell, is present to condition power from the TEGs. In this test system, the TEGs and power conditioning board are wired directly to external monitors through electrical passthroughs, allowing direct performance of the components to be measured. Additionally, local temperature gradients across the device were monitored using Iconel-sheathed thermocouples.

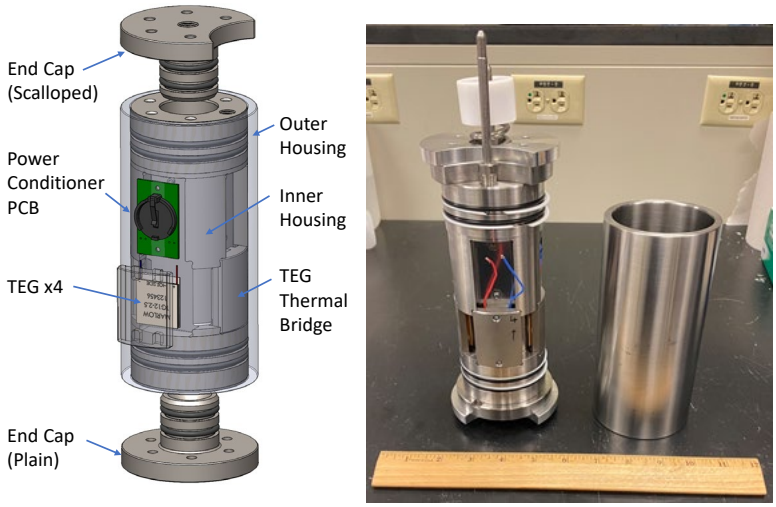

Figure 3-2. Prototype high pressure power generation module for benchtop testing. Left: schematic with endplates installed for benchtop testing. Right: fabricated test unit.

Initial testing with the lab prototype was aimed at demonstrating proof of concept and was done under low pressure conditions by flowing a cold aqueous solution through the central "tube" and heating the device externally. Thermocouples were mounted directly on the outside of the assembly, on the inside wall next to where the TEG is housed, and then on the inside of the flowing tube. Upon achieving steady state, with the flowing solution inside at 6–7ºC, the outside boundary at ~65–70 ºC, and the inner wall at 28ºC, the open circuit voltage from one TEG array read ~ 236 mV. The millivolt reading, measured with a data acquisition device, was verified with a multimeter, and all three TEG arrays on the device read the same mV output. An earlier experiment without flowing cold solution gave an output of ~90 mV, with a ~ 30ºC difference between the outside and adjacent walls. Thus, power was generated from the device "as-is" but it was much less than anticipated for a given thermal gradient (Figure 3-3). This was attributed to heat flow around the TEGs, through the legs of the fixtures that hold the TEGs and the screws that hold the thermal bridges in place, and to poor thermal coupling at the various interfaces—e.g., air gaps at the interfaces—were creating a thermal resistance such that a thermal by-pass was developing around the thermopile arrays.

Thermal imaging during the test (Figure 3-4) was used to confirm that heat was bypassing the TEGs. The prototype, with its outer shell removed to allow access to the TEGs, was coated with black electrical tape to increase emissivity and improve image contrast. Heated water (70°C) was then circulated through the central cavity. A thermal camera was then used to image the system as it heated up. The results confirm that the thermal bridges above the TEGs heated up rapidly due to

conductive heat transfer through the legs of the caps to the top, circumventing the TEG assembly below the bridge.

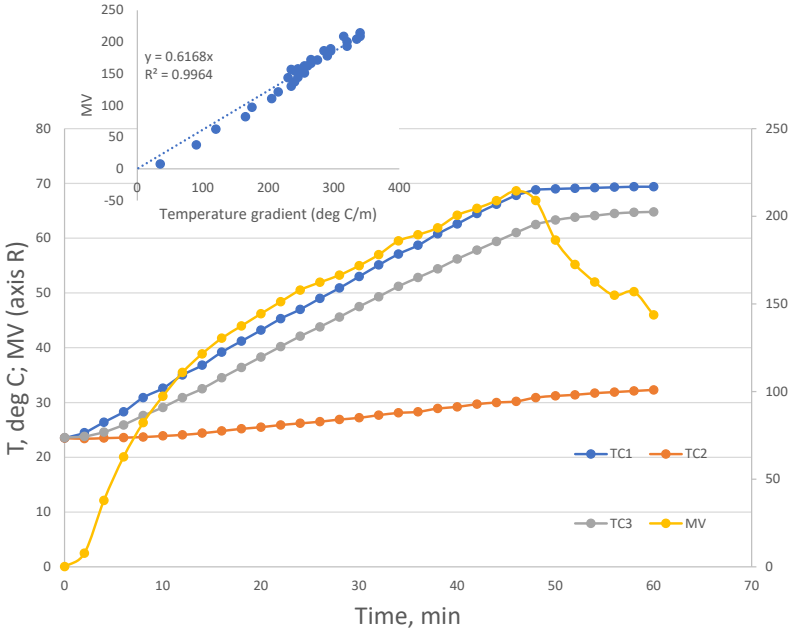

Figure 3-3. Temperatures at different locations in the prototype during a thermal test. TC-1 — inside orifice; TC-2 — on upper part of assembly, but thought not to be in contact; TC-3 — between TEG element and inner wall. Also shown are millivolts produced by the TEG, and the voltage produced vs the apparent temperature gradient (inset).

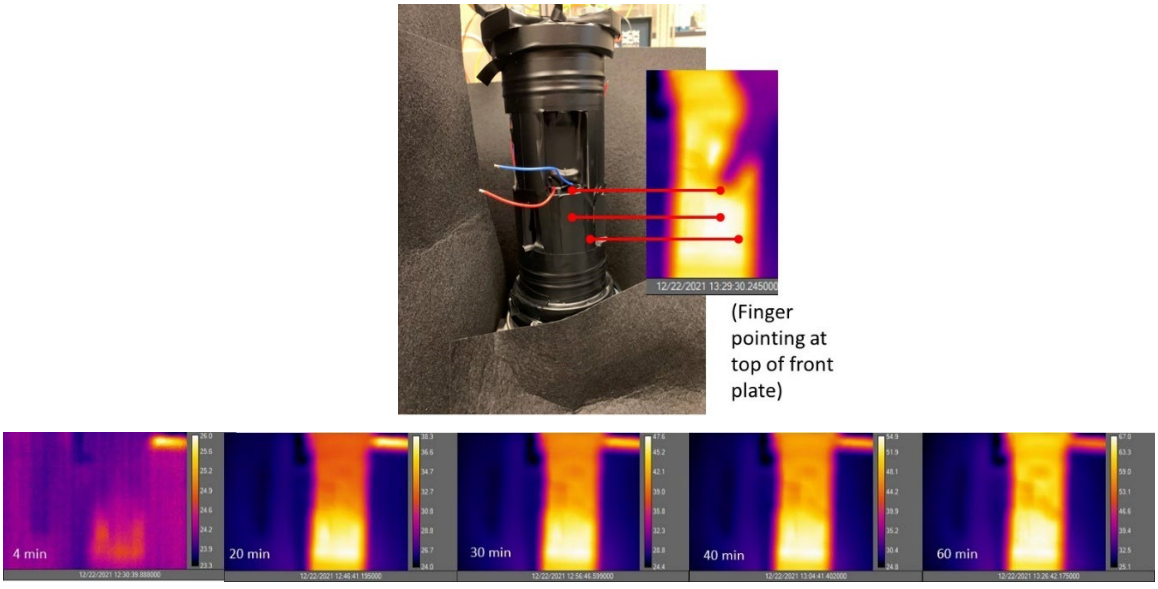

Figure 3-4. Thermal imaging of laboratory prototype during a heated flow test.

Diagnostic thermocouples were placed on various surfaces to better understand the heat losses at the interfaces and help optimize the design to maximize the ΔT across the thermopile. Thermal modeling was also used to evaluate the heat flow pathways, and to optimize the design. Design modifications were made to improve thermal coupling at interfaces, and other regions of the device were insulated to help channel more heat through the thermopile arrays; thermally isolating the hot and cold side cover plates and the assembly should the ΔT across the thermopile and yield higher power output. Of particular importance was to minimize heat flow around the TEGs to maximize heat flow through the TEGs, and the thermal bridges were redesigned to accomplish this. New polymer fixtures were built to replace the legs and retaining screws of the cap, and thermal transfer between the caps and the outer shell was increased by replacing the steel caps with higher thermal conductivity aluminum ones. In addition, flexible fins extending from the cap ensure good thermal contact with the outer shell. The gaps between the fins can be filled with thermally conductive grease. The Version 2 thermal bridge assembly is shown in Figure 3-5. The assembly consists of a 6061-T6 aluminum TEG thermal bridge with flexible heat flow elements, a Garolite G10/FR4 insulated fixture to hold the TEG in place, and the TEG itself.

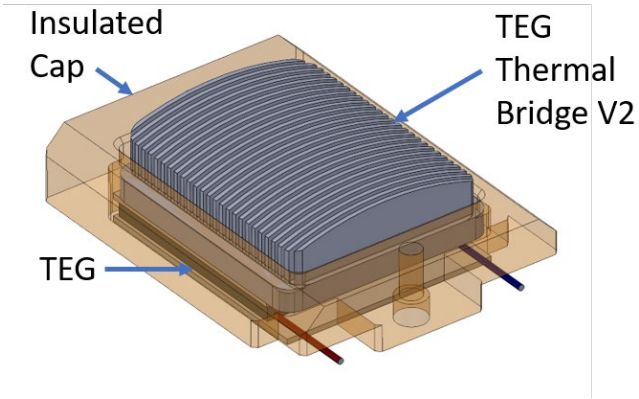

Figure 3-5. Version 2 TEG thermal bridge assembly.

Although the Version 2 thermal bridge and cap improved heat flow, they were not ideal; the fins had been designed to be slightly larger inner radius of the shell, such that they would flex when the unit was assembled, and the outer shell was slid over the inner assembly. However, the fins were too rigid—sliding the outer shell over the assembly proved to be very difficult, requiring a press. When the unit was assembled for a high-pressure test, sliding the shell over the thermal bridges damaged the TEGs underneath, and the inner assembly was badly scored. The damage to the inner assembly prevented high pressure lab tests from being carried out on the lab prototype, as it interfered with the seal of the O-rings. Funding and schedule constraints did not permit machining of a new prototype, so high-pressure tests were not possible. However, the damage prototype was still useful, as it could still be used to optimize component designs. In particular, a new thermal bridge was designed.

In the final design (Version 3), the same materials are used for the bridges, but the thermal bridges are two-part. A finned bottom plate is placed on top of the TEG, and then a second, spring-loaded plate with interfingering fins is placed on top. The spring-loaded plate readily compresses when the inner housing is inserted into the outer shell, allowing easy insertion; however, the spring also presses the upper plate against the outer shell, maintaining good thermal contact. Thermal grease is

used to maintain good thermal contact between the interfingered fins on each half. The upper and lower plates of the Version 3 thermal bridge assembly are shown in Figure 3-6.

The Version 3 thermal bridges were very effective, being easily inserted, and working well to channel heat through the TEGs. This is illustrated in Figure 3-7, which shows results of a test flowing hot water through the prototype vessel central annulus. Figure 3-7A, shows the response of thermocouples placed on either side of a single TEG element, inside the vessel annulus (with flowing hot water), and outer surface of the vessel. With progressive heating, the generated temperature gradient induces a voltage of about 0.5 V from a single TEG element, which is sustained as the vessel heats up from the inside. Figure 3-7B shows that the generated voltage is linearly proportional to the induce thermal gradient; the infrared images of the prototype vessel taken at various stages throughout the testing show a higher temperature on the vessel exterior directly outside the location of the TEG caps. A similar test run without the outer shell (which dissipates heat through air and not through thermal contact between cap and outer shell) only produced a temperature gradient of ~ 7.4 °C across each TEG element, with a commensurate drop in voltage produced per element of about 0.2 V.

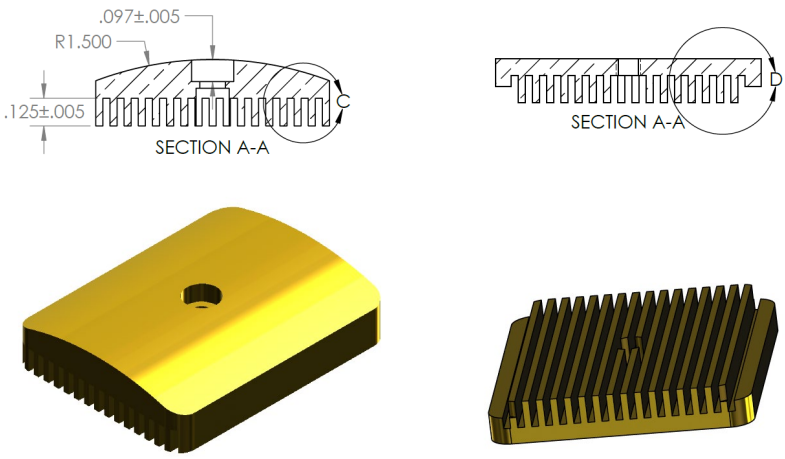

Figure 3-6. Version 3 TEG thermal bridge assembly, with the upper plate on the left and the lower plate on the right.

As note previously, the Version 3 caps were very effective, being easily inserted and working well to channel heat through the TEGs. This is illustrated in Figure 3-7, where we show results of a test flowing hot water (~75°C) through the prototype vessel central annulus (an analog for production or injection tubing inside a wellbore). In Figure 3-7A, we show the response of thermocouples placed on either side of a single TEG element, inside the vessel annulus (with flowing hot water), and outside the vessel. With progressive heating, the generated temperature gradient induces a voltage of about 0.5 V from a single TEG element, which is sustained as the vessel heats up from the inside. Figure 3-7B shows that the generated voltage is linearly proportional to the induce thermal gradient; the infrared images of the prototype vessel taken at various stages throughout the testing show a higher temperature on the vessel exterior directly outside the location of the TEG caps. A similar test run without the outer shell (which dissipates heat through air and not through thermal contact between cap and outer shell) only produced a temperature gradient of ~ 7.4 °C across each TEG element, with a commensurate drop in the voltage produced per element to about 0.2 V. These

tests showed that the Version 3 caps and thermal bridges were effective at directing heat flow through the TEGs, and they were chosen for the field prototype.

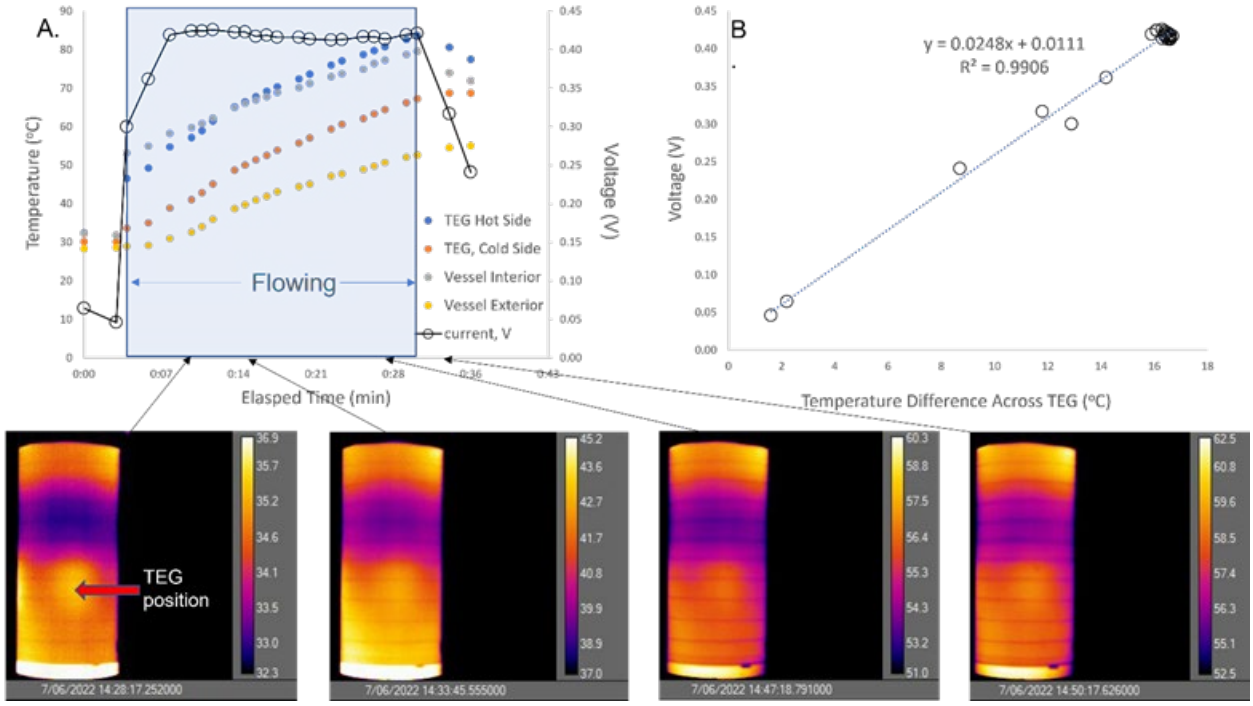

Figure 3-7. A. Results of flow-through heating test of the prototype fitted with the version 3 TEG caps. The data points in the figures show the temperatures measured by thermocouple placed on either side of a TEG element, and inside and outside the prototype vessel, as ~75 ºC water was flowed through the central tube of the prototype. B. The increase in temperature gradient across the TEGs with progressive heating results in a linear increase in the produced current. Thermal images along the bottom confirm that the new TEG caps focus heat flow more efficiently, with the device generating almost 0.5 volts per TEG array for approximately 30 minutes.

Although the damage to the lab prototype did not allow a high-pressure test to be carried out, the lab prototype was important in optimizing several components of the pressure harvester to maximize heat flow through the TEGs and power generation. Moreover, it allowed testing of the electronics as a complete package. Finally, the lab tests were important in determining the necessary size (number of TEGs) required for the field prototype. The low power generation observed with the Version 1 thermal bridges suggested that 40 TEGs might not be sufficient for the field prototype, and 80 would be a safer number. However, the heat flow and power generation with the Version 3 bridges was much higher, indicating that 40 TEGs would be more than sufficient for charging the battery under anticipated field conditions, either for the field test, or for a real borehole environment. On the basis of this, the dimensions of the field prototype were determined.

4. Designing and building the field prototype

The overall approach for the field unit reflected that of the laboratory unit. A schematic for the field prototype is shown in Figure 4-1. As with the laboratory prototype, it consists of a machined inner housing that holds a series of TEGs, a PCB, and a battery within an outer protective sheath. this design is simply an expanded version of the laboratory prototype and can be further extended to incorporate more TEG modules if necessary. This unit has an American Petroleum Institute (API) standard box and pin welded to the ends and is intended to be installed in-line within the tubing string and emplaced at the desired depth. The inner diameter of the power harvester matches that of the tubing, to the degree possible, to avoid impacting pumping pressures during injections.

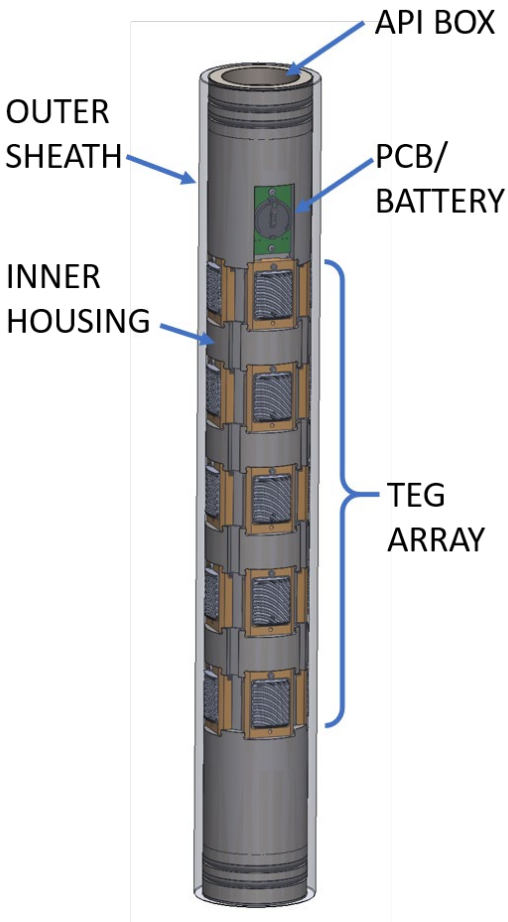

Figure 4-1. Schematic of the field deployable thermopile energy generation system.

4.1. Determining power harvester specifications

In order to finalize the design of the power harvester field prototype, it was first necessary to determine the anticipated conditions in a scCO2 injection well, at the depths of interest, during a typical injection cycle. It was also necessary to determine the required dimensions for the tool, as constrained by the borehole geometry. Since SNL has been an active team member of the SWP, a conversation was initiated with the lead organization, the New Mexico Institute of Mining and

Technology (NMT), to both obtain necessary field condition information and to discuss the possibility of collaborating to carry out a field demonstration of the unit. The team interacted with George El-kaseeh, an employee of the Petroleum Recovery Research Center at NMT and the coordinator of field activities for the SWP Farnsworth Unit CO_2 Storage-EOR Project. The SWP supplied a well inventory for the western portion of the Farnsworth Unit where SWP focuses its studies, with wellbore diagrams and data on cement type, casing type/sizes, production or injection volumes, and similar information. The team also had access to a variety of core testing data and well logs (e.g., caliper logs) from the existing collaborations—two team members (Thomas Dewers and Jason Heath) have been participants on the Site Characterization Group of the SWP (e.g., see Wu et al., 2020; Heath et al., 2021; Moodie et al., 2021; Trujillo et al., 2021; Simmons et al., 2022).

Discussions with the SWP resulted in the development of a detailed parameter list. Parameters were identified that relate to initial conditions, boundary conditions, material properties of the wellbore, the host rock, and the TEGs. Key parameters for design of the include well geometries. Wellbore diagrams and well drilling reports provided casing and tubing sizes (ID, OD), which are necessary to design a compatible power harvesting tool that can be inserted into the casing on the tubing string. Moreover, injection and production data were used to estimate the timing, temperatures, and pressures associated with $scCO_2$ injection pulses. These were critical parameters for defining the power harvesting tool design specifications for temperature and pressure and are also necessary to accurately size TEG arrays and to accurately model and estimate available power under field conditions (e.g., water-alternating-gas schedules for CO_2 storage-EOR scenarios or other fluid-pulse scenarios for non-EOR storage-only sites; realistic reservoir pressure and temperature variations in space and time based on field data). Additional parameters include thermal properties for various wellbore and wall rock components. All of these are necessary both to design the power harvesting instrument, and for lab- and field-scale modeling of power generation under realistic changing fluid conditions and associated thermal pulses.

Ultimately, liability requirements imposed by the site operator for the proposed field test eliminated the SWP Farnsworth site as a possible test site. However, all well parameters (casing and tubing dimensions, injection and production schedules, downhole temperatures and pressures) used to design the power harvester and plan the final field unit testing at a commercial downhole and pressure vessel testing facility (see Section 5) are based on a SWP injection well at the Farnsworth Unit. The well is typical of CO_2 injection wells, and at the reservoir depth, the casing has an outer diameter of 5.50" and an ID of 4.775"—the team learned that the thermopile field unit should not have an OD larger than 4.0″. The production composite lined tubing has an OD of $2\,^{7}/_{8}$" and an ID of 2.25". The laboratory and field prototypes of the power harvesting unit were designed to be consistent with these dimensions, with the inner diameter generally matching or similar to the inner diameter of the tubing to the degree possible to minimize back-pressure, and with the outer diameter leaving sufficient clearance with the casing to allow safe insertion and removal from the borehole (hence the recommended 4.0″ size).

Pumping schedules from the site were also used to define the relevant pressure requirements for the tools. Using pressure information from near to or at the reservoir depths at Farnsworth, the team estimated for a power harvesting tool on the tubing string that it should be designed to withstand an external pressure of 3,000 psi and an internal pressure during an injection cycle of 6,000 psi. The laboratory and field prototypes were designed to operate under these conditions, with substantial safety margins. Reservoir temperatures at Farnsworth are about 70ºC; to provide some margin, the prototypes were designed to operate up to at least 80ºC, the limit being induced by limitations in the electronics.

4.2. COMSOL modeling to determine the necessary size of the field prototype

COMSOL modeling was carried out to determine anticipated heat fluxes through an emplaced prototype in the downhole setting, caused by thermal pulses associated with supercritical CO_2 and water injections (Figure 4-2). This modeling was done to evaluate power generation by each TEG, necessary to determine the number of required TEGs and hence, to size the field prototype.

To explore thermal responses under field conditions, we ran a simple 2D axisymmetric simulation of heat flow associated with injection of surface temperature water for eight-hours with a 40-hour recovery period (Figure 4-3). As a method for determining the heat flux associated with injecting cold water from the surface via a borehole, the following expression was used:

$$Q_l \text{ (Watts/m/K)} = C_{pw} M_l (T_{inj} - T),$$

where Q_l is the heat line source/sink within the wellbore, C_{pw} is the heat capacity of water, M_l is the mass flow per unit line length (equal to 10 kg/m/s), and T_{inj} is the injection temperature (15°C). A geothermal gradient of 30°C/km, a 0.1 m wellbore radius, and an eight-hour injection period were assumed. This model provides heat fluxes and temperature distributions that can be used to estimate thermopile power generation in down-hole conditions.

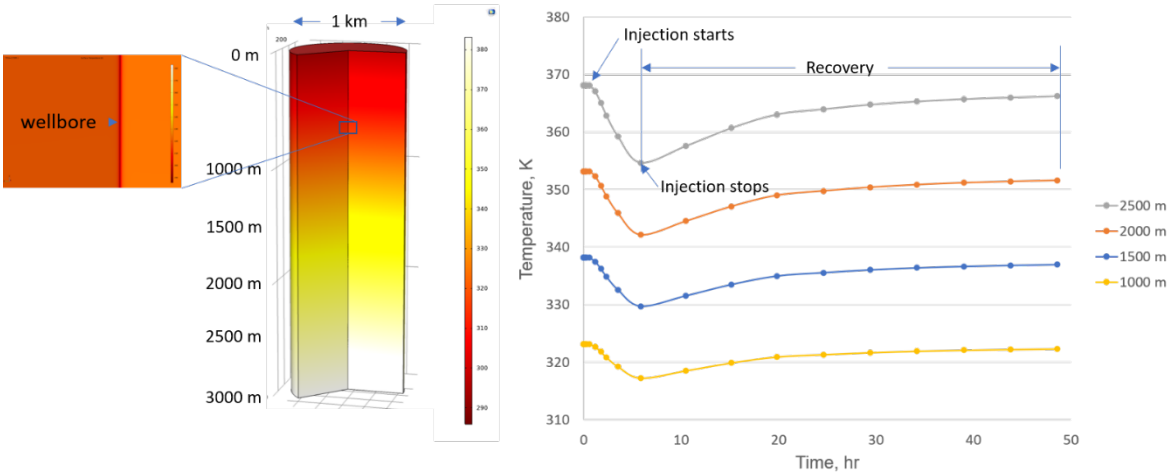

Figure 4-2. Thermal modeling of surface water injection for an eight-hour injection period followed by a 40-hour recovery period. The simulation domain is a 0.5 km radius cylindrical domain and solves for temperature assuming axisymmetry around the wellbore. The right-hand figure shows temperature at a distance of 0.1 m from the wellbore center line at four different depths (the proposed depth for the testing falls in between the 2000 and 2500 m locations).

Using measurements of power efficiency from the laboratory prototype and the estimated of thermal gradient from the modeling, it was determined that 40 TEGs would generate sufficient power for the field test, and the field prototype was sized accordingly.

4.3. Field site

While the data from SWP provided the desired specifications for the power harvester and modeling provided information necessary to specify the number of TEGs required. Other test-specific design

parameters such as the OD of the tool required identifying a test site and actual borehole for the field test and developing a field test plan. The most important of these is the ID of the casing, as this places hard limits on the diameter of the tool. Also, the required fittings for coupling to on-site equipment are site- and test-specific. Final design steps were delayed until a field site and test plan could be developed.

After months of effort, discussions for a field test with SWP came to a halt, when the Farnsworth site operator imposed requirements for the test that Sandia could not meet. A search for a new site was initiated. Three commercial well-testing companies were contacted—the Catoosa Test Facility in Hallett, OK; the Quest Test Facility in Stillwater, OK; and APS Technology Drilling Test Facility in Wallingford, CT. Discussions were also carried out with the University of Texas Devine test site. None of these sites have capabilities for CO_2 injection, and none have wells test wells deeper than approximately 3000 feet. Hence, discussions focused on doing shallower tests and creating a thermal gradient by circulating heated water. The APS Wallingford site offered, in addition to a shallow well for a circulating fluid test, a pressure vessel test for evaluating tool survivability at realistic pressures and temperatures for CO_2 injection. APS-Wallingford also had the necessary equipment on-site and boreholes of sufficient casing diameter such that no significant tool redesign was required. For these reasons, APS-Wallingford was chosen for the field test. This choice has additional benefits, as APS has a good deal of expertise in borehole tool testing and was able to suggest several minor improvements to the tool and to the planned field tests. Working with information supplied by APS, a final prototype design, including end-caps for specific tests to be carried out at APS, was developed.

4.4. Final field prototype design

An engineering drawing of the final version in shown in Figure 4-3. As with the lab prototype, the field deployable unit consists of a machined inner housing that holds a series of TEGs, a PCB, and batteries within an outer protective sheath. It is designed to hold ~ 40 TEG assemblies and is 42 inches long. This design can be further extended to incorporate more TEG modules if necessary. The field prototype incorporates the Version 3 thermal bridges and several other design improvements to facilitate ease of assembly. The final design specification incorporated finite elemental analysis for strength performance to ensure that safety margins were met. Both pressure requirements and possible applied torques during attachment to the casing string were considered.

The configuration shown in Figure 4-3 is specific for testing at the APS Technology test facility. Additional configurations can be achieved through variations in the end adapters as shown in Figure 4-4. The as-built version can accommodate up to 40 TEG modules, but for power generation in a real $scCO_2$ injection well, can be readily lengthened to any length up to the entire length of a joint of tubing (up to 32 feet in length).

The end-caps for the two field tests are shown in Figure 4-4. The upper end-cap has an eye bolt for suspending the tool in the pressure vessel for the pressure test, and in the borehole for the flow test. In the pressure test, a small port will allow access for pressurizing the inner tube of the vessel, to simulate downhole conditions. A larger port in the cap will be sealed. The lower cap also has sealed port, which will be plugged for the pressure test. For the down-hole flow test, the large ports on the upper and lower end-caps will be attached to tubing, and hot water will be circulated through the tool to create a thermal gradient. To maintain the thermal gradient for the duration of the test, cold water will be pumped down the annulus of the well around the tool.

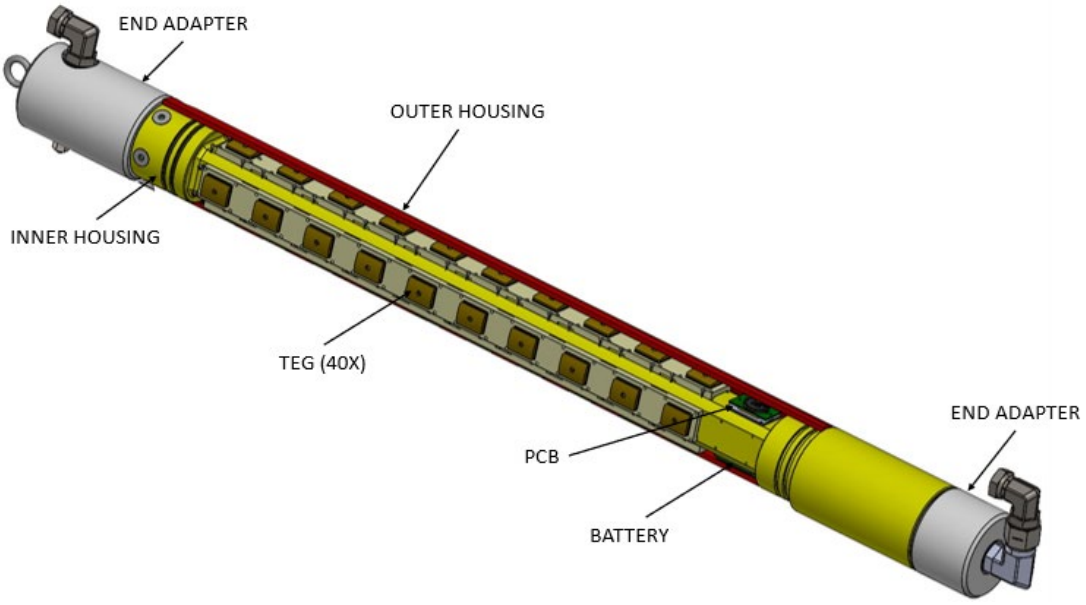

Figure 4-3. Schematic of the field deployable thermopile energy generation system.

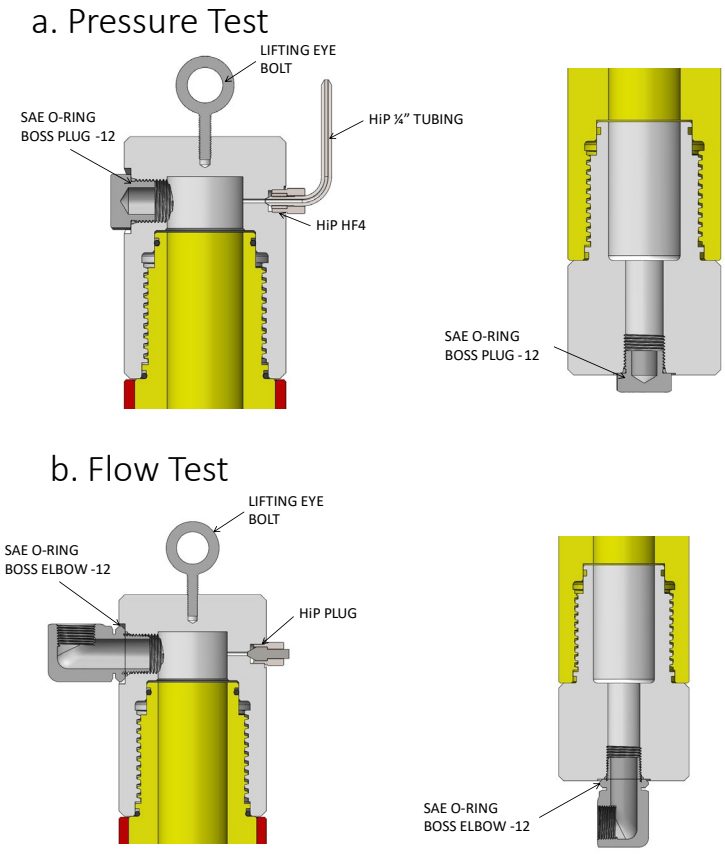

Figure 4-4. Engineering sketches of the end-caps for (a) the pressure vessel test; and (b) the flow (wellbore) test.

4.5. Field prototype assembly and testing at SNL

The fabricated inner assembly and outer shell were delivered to SNL at the end of October, 2022, and a preliminary assembly was carried out to test clearances (Figure 4-5) The bare inner assembly is shown in Figure 4-5A and the installed TEGS and thermal bridges are shown in Figure 4-5B. Note that the spring-loaded thermal bridges are designed to tilt slightly to facilitate sliding on the outer sheath; they then snap into place. The partially installed outer sheath is shown in Figure 4-5C, and the closed unit, with the outer shell completely in place, is shown in Figure 4-5D.

The fully populated inner assembly is shown in Figure 4-6. The field prototype was then fully assembled and tested as a unit. In this test, hot air was blown through the unit to create a thermal gradient and confirm power generation. Prior to shipping to APS for the field tests, the battery was partially charged, so that there would be no delay in recording data once testing began.

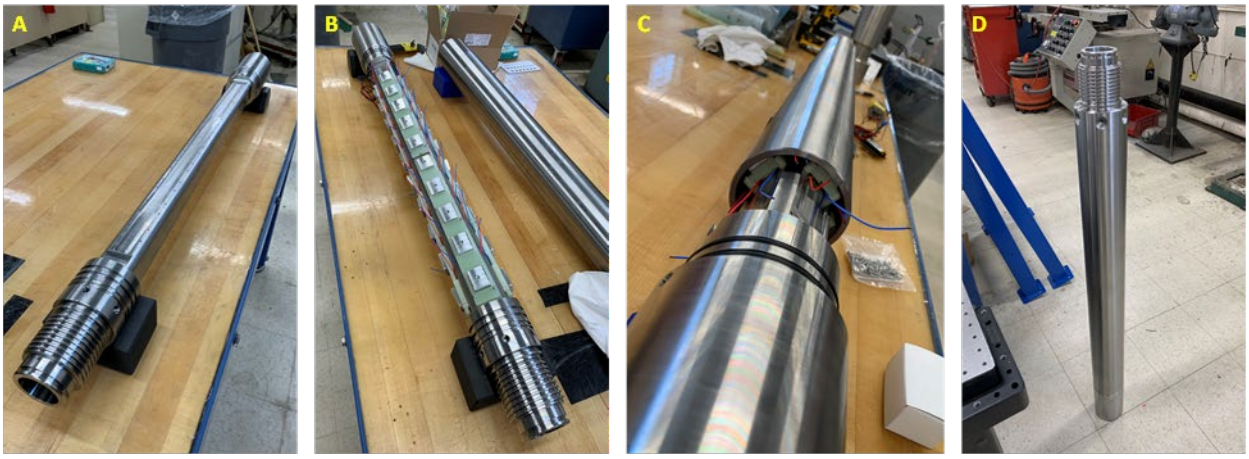

Figure 4-5. Preliminary assembly of field prototype energy harvester to test clearances. A) Bare inner assembly. B) Inner assembly with TEGs and thermal bridges in place. C) Sliding the outer shell the thermal bridges. D) Unit with outer shell fully in position.

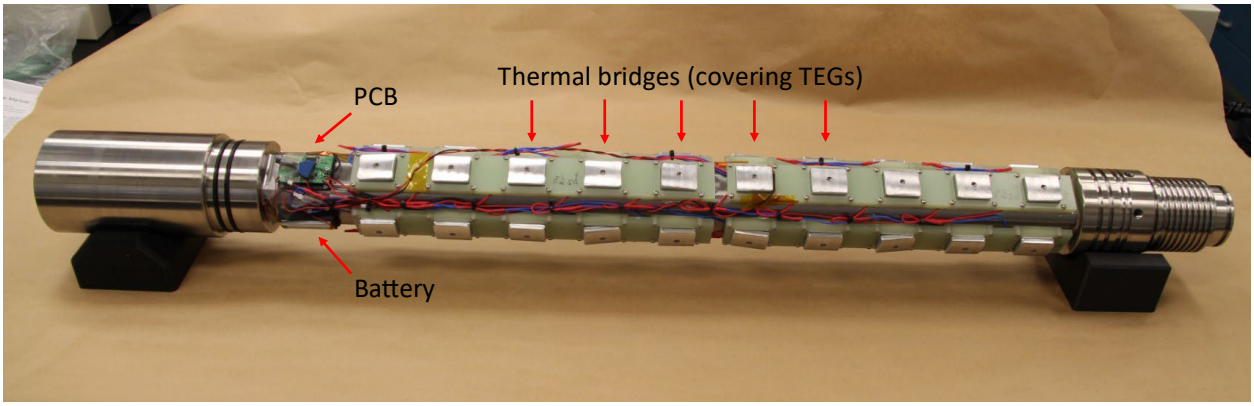

Figure 4-6. Fully wired inner assembly, with TEGs, thermal bridges, PCB, and battery.

To evaluate the efficiency of the power generation, the thermistors attached to the PCB were placed at three positions. T_0 was placed against the inner shell, 7.2″ from the upper end of the inner assembly (the "hot side" for the TEGs); T_1 was placed at the same distance, but on the inside of the outer shell (the "cold side" for the TEGs); and T_2 was placed 26.6″ further down, against the inner shell (Figure 4-7). The ΔT was calculated as T0-T1, while T0 and T3 were compared to determine how much the temperature varied along the length of the power harvester.

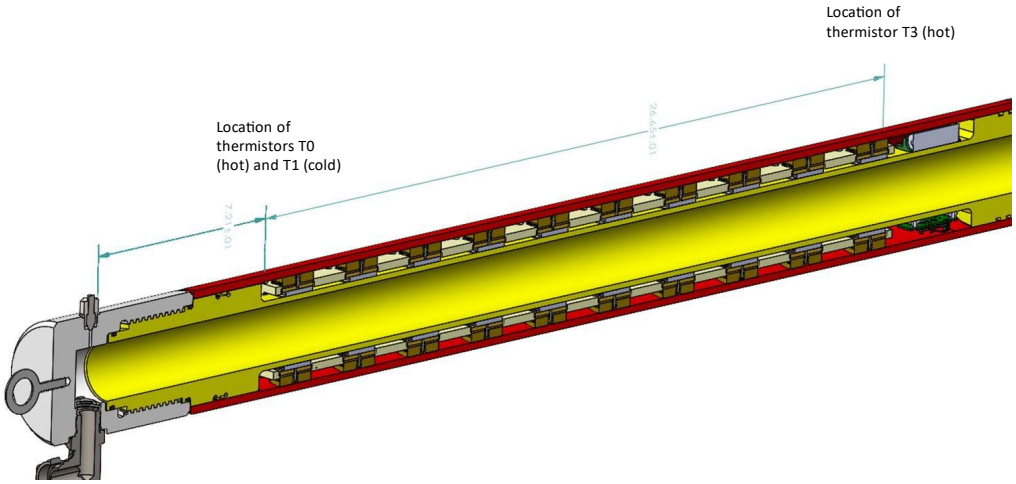

Figure 4-7. Location of thermistors on the power harvester field prototype.

5. Field test

Sandia personnel traveled to APS the week of November 30th, 2022 to assist and guide the field test sequence. As described previously, three separate test sequences were planned at the APS facility at Wallingford, CT. The first test failed, wherein a leak at the helium leak testing port allowed water to flow into the tool, in effect shorting out the instrument electronics as shown by the retrieved data. This failure point was corrected onsite at APS, and the two subsequent tests were successful, demonstrating downhole current generation from circulating hot fluid, and pressure survivability, with current generation accompanying heating of the tool within a pressure vessel. These tests are detailed below.

5.1. Test plan

The planned demonstration testing of the TEG tool at APS involved two distinct types of tests. The first (Well Testing) involved placing the tool into a shallow wellbore surrounded by Triassic sandstone formations. Hot water was to be circulated through the tool to simulate the production of deeper hotter fluid, and data on current generation from the induced thermal gradient was to be recorded on board the tool, and subsequently retrieved at test conclusion when the instrument was brought to the surface. The heat flux in this experimental setup is from inside-out, opposite to that expected in a CO_2 injection scenario, but this modification simply required reversing the leads running from the serially wired TEGs to the power conditioning board.

The second test (Pressure Vessel Test) involved placing the tool in a pressure vessel, inducing pressure conditions simulating an injection scenario observed from the SWP at Farnsworth, TX, and then heating the tool to subsurface conditions. Data on current generation was to be stored on board the instrument to be retrieved at the conclusion of testing. It was decided to perform the well testing first, such that any failure of the instrument from high pressure testing would not preclude subsequent wellbore testing.

The *initial test plan* developed for the two types of tests is as follows:

Well Testing

- Tool Weight: 150 lb. estimate
- Perform He leak test
- Connect hot water supply and return fittings and tubing, secure to the OD of the tool
- Hot water enters uphole end
- Return water leaves downhole end
- Circulate hot water thru tool while in the formation
- Max water temperature supply to the tool = 80 °C (176 °F)
- Achieve delta T of 9 °F to 19 °F
- Circulate water at approximately 2-4 gpm
- Monitor borehole fluid temperature
- Monitor hot water temperature entering the tool (80 °C max)
- Test duration: two days
- Test cycle: two 4-hour cycles
- Tool will be in memory mode only – no power or external instrumentation required
- Monitor and record borehole water temp, supply water temp, return water temp
- Partially remove outer housing, dump on board memory and reset, reassemble

Pressure Vessel Testing

- Interior pressure equal to 6,000 psi
- Exterior pressure equal to 3,000 psi
- Torque and seal endcaps
- Perform He leak test to demonstrate tool sealing
- Suspend the Thermopile tool to the pressure bomb head with chain.
- Fabricate the HiP HF4/HF4 connecting tube to be used in pressurizing the interior of the tool
- Install the connecting tube and torque fittings
- Lower the pressure head/thermopile tool into the pressure bomb
- Secure the pressure head for 6,000 psi/150 °C operation. (0.3 × Torque)
    - Heat cycle: two cycles room T - 80 °C – room T, one cycle per day
    - Pressure cycles: two cycles 6,000/3,000 psi per day, max 500 psi /min
    - Duration: hold at 6,000/3,000 psi for 2 hours

In the next section, the results of this testing plan are presented, and the behavior of the downhole system in generating current during fluid injection and extraction is discussed.

5.2. Test results

Ultimately, three tests were carried out at the APS Technology test site, two wellbore tests, and one high-pressure survivability test.

5.2.1. First wellbore test

Sandia shipped the TEG instrument to APS with an extra on-board electronics and battery, which proved premonitory, as the First Wellbore Test resulted in a flooding of the internal tool (with electronics) with water, resulting in a short and a failed test. Figure 5-1 shows the instrument as received at APS, downloading data from the onboard electronics and setting the data acquisition rate, and then undergoing an initial helium leak test at APS.

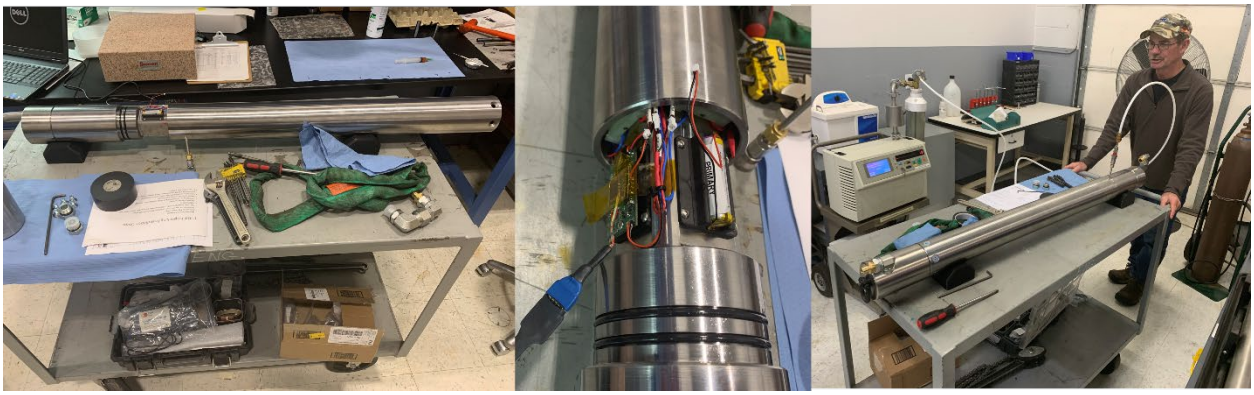

Figure 5-1. From left: Prepping the instrument for the initial wellbore test; initialization of the onboard electronics; helium leak test.

The initial helium leak test proved successfully, demonstrating that the O-ring seals in the instrument were successfully holding against an external positive pressure. The instrument was then moved to the borehole laboratory at APS, which contained several shallow wellbores designed for borehole tool testing. APS personnel had in place a water reservoir connected to a propane water heater that could supply heated water to ~80°C at gallons per minute rates. Three external thermocouples were attached to the tool assembly, one on the injection tubing close the tool inlet, one on the injection tubing close to the tube outlet, and one on the tool assembly away from the tubing, to gage downhole temperature change associated with warming from the tool assembly. These were monitored throughout the two borehole tests. The tool was then lowered into test borehole, along with fluid injection ad extraction tubing and wiring for the external thermocouples (Figure 5-2).

Figure 5-2. (Left) Water reservoir, propane heater, and pump used to simulate hot fluid extraction to gauge instrument response to the induced thermal gradient. (Center) Instrument is lowered into the borehole. (Right) Fluid injection and extraction tubing and thermocouple wiring is lowered into the wellbore to an approximate depth of 62.5 feet (from top of well to top of tool), into Triassic sandstone bedrock.

The following day, the tool was extracted from the wellbore and brought into the lab for data extraction. It was here that it was discovered that the tool had leaked; borehole water had entered the tool and shorted the electronics. An investigation revealed that the helium test port for testing the O-ring seals had been incorrectly tapped; the port has worked during the He leak test but had not sealed properly when the shorter plug was inserted for the downhole test (Figure 5-3). However, APS has a fully equipped fabrication/machining facility, and they were able to re-tap the hole, fixing the problem. The tool was dried and prepared with the replacement board and battery for testing the following day.

Figure 5-3. Comparison of the He probe tip and the He port plug. The tapped threads had to be extended deeper into the port for the plug to properly seat and seal the port.

The three external thermocouples were monitored during the entire test and the outputs are shown in Figure 5-4. Despite the exposure to moisture, we were able to extract usable data off the board (Figure 5-5) which shows that the leak was slow enough that the initial pumping of hot fluid into the vessel was captured before the board shorted. Figure 5-5 shows the initial increase in temperature measured by the on-board electronics, and a commensurate increase in generated current by the induced thermal gradient, just before the chamber became flooded.

Lowering the tool into the well, it was noticed that a small current was generated when the tool reached the water table at approximately 16.3 feet from top of casing, noted by an instant drop in thermocouple, at about 58 minutes into the test (Figure 5-5). Once the tool reached the maximum depth of 62.5' from top of casing, hot water pumping into the too was initiated at about 79 minutes into the test. As shown both by the external thermocouples (measured in real time shown in Figure 5-4) and on-board thermistors (Figure 5-5) the generated current responded almost instantaneously to the induced temperature gradient at around 80 minutes (Figure 5-5, yellow curve). This pumping was sustained with slight adjustments to the injected water temperature, evident from the small variations seen in the water temperatures in the initial part of the test (Figure 5-4). After two hours of pumping, the injection was halted and the temperature within the wellbore was allowed to slowly cool, as evidenced by the long tail decline observed in Figure 5-4, which occurred over approximately 15 hours.

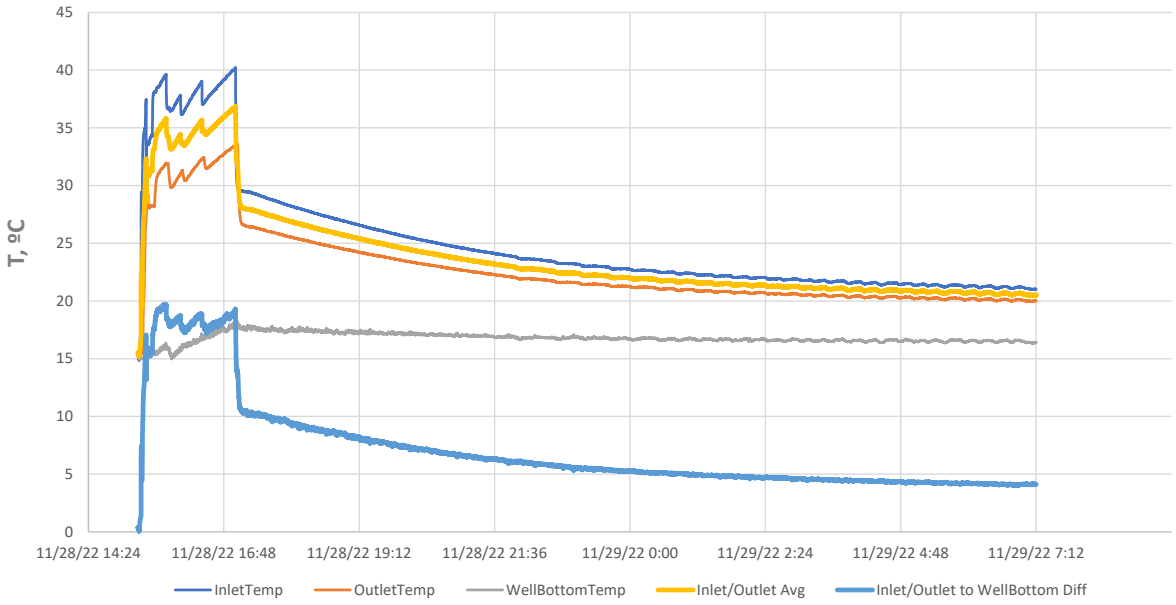

Figure 5-4. External temperatures measured by thermocouples placed at the fluid inlet (thin blue line), fluid outlet (thin orange line) and middle (grey line) of the TEG tool. The middle thermocouple extended out away from the vessel and measured wellbore temperature. The thick yellow and blue lines indicate the average of the inlet and outlet temperature, and the difference of this average and the measured wellbore temperature, respectively. The temperature indicated by the blue line is proportional to the thermal gradient and is thus an indicator of the current generated by the tool. The temperature patterns show the impact of heating by injected hot water for approximately 2 hours, followed by a long cooling period of approximately 15 hours.

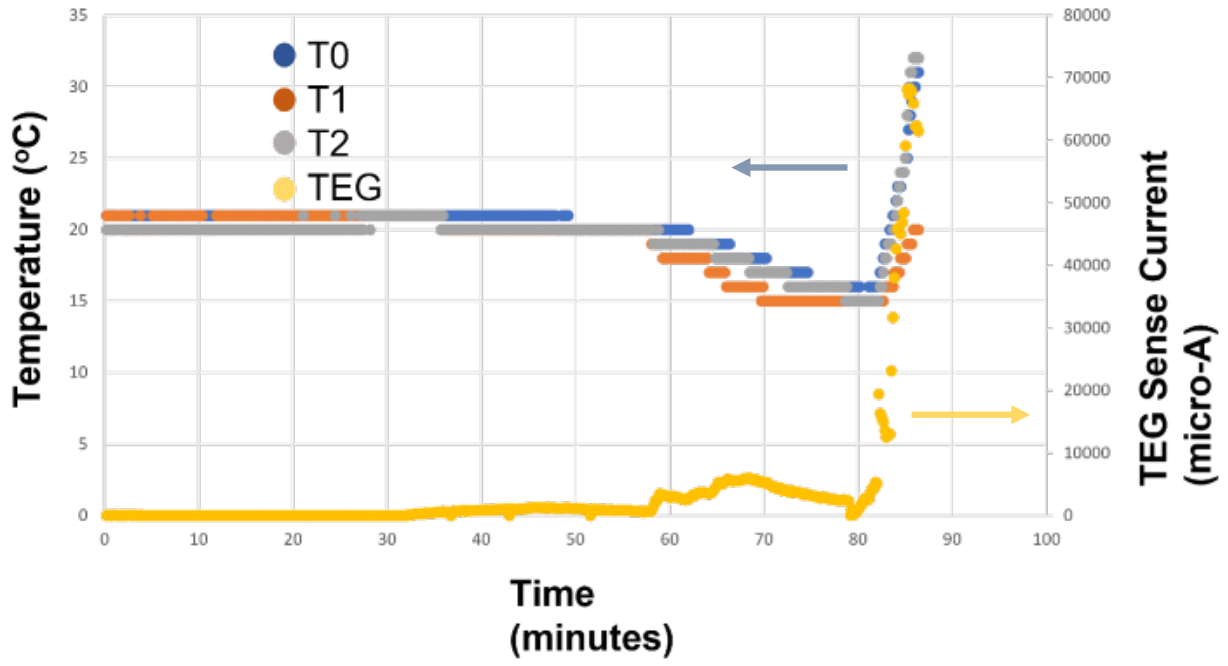

Figure 5-5. Changes in internal thermistor temperatures (T0, T1, and T2) and TEG sense current (yellow curve, right hand vertical axis) during Wellbore Test 1. Time 0 is when the tool was sealed; the next 30 minutes correspond to when the tool was undergoing a helium leak test. At ~35 minutes, the tool was hoisted to the wellbore laboratory, resulting in a slight cooling at about 35-40 minutes (and generating a small current from ~35 to ~55 minutes). The vessel was lowered into the wellbore and encountered the water table about 16.5 feet below top of casing, indicated by the rapid decrease in temperature and a slightly larger generated current between ~58 to ~ 80 minutes. At 80 minutes, hot fluid injection commenced, resulting in notable increase in generated current. The on-board electronics shorted due to fluid leakage at ~ 86 minutes.

5.2.2. Second Wellbore Test

After replacing and testing the PCB and battery, and drying the internal regions of the tool, the tool was reassembled for a second wellbore test the following day. The procedure was exactly the same as in the First Wellbore Test. First, the board data was cleared and the battery was hooked up, and then outer shell was placed and the tool was subjected to a helium leak test. This was followed by lowering the tool back into the wellbore (Figure 5-6) and commencing with injection of heated water. For this test, given the failure of the first wellbore test, we decided to run an abbreviated test wherein we pumped heated fluid with increasing temperature to gauge the response of the TEG elements to a stepwise increase in temperature gradient (Figure 5-7 and Figure 5-8). The test was run in four different stages, increasing the ΔT across the thermopile at each stage. The stages are shown in Table 5-1, but it should be noted that the values provided are only approximate, as steady state was only achieved in Stage 1. In the other stages, the temperatures were still rising increasing when the stage ended. The temperature data were measured using the thermistors attached to the PCB. The test lasted approximately 6 hours and involved four pulses of heated water each lasting approximately 40 minutes. Data was recorded by the PCB at a rate of once per minute. Figure 5-7 shows the temperature response of the thermocouples positioned outside the immersed tool and monitored from the surface, and Figure 5-8 shows the response of the internal thermistors and the generated current. Data were collected for the entire duration of the test, and there is good correlation between the TEG generated current and the induced temperature gradient across the

cross section of the tool. As the ΔT increased in each successive stage, the level of power generation increased. At the lowest ΔT of 5ºC, the unit was generating about 10 mA of current, which was acceptable for charging a battery.

Figure 5-6. From left: Lowering the renewed tool into the experimental wellbore; Hot and cold hoses inside the wellbore at lower left; APS staff monitoring the thermocouple response (foreground) and heater temperature (background); extracting the tool at the end of the test.

Table 5-1. Heating stages in the down-hole power generation test.

Stage #	T0 (hot), ºC	T1 (cold), ºC	ΔT, ºC
1	24	19	5
2	29	21	8
3	36.5	25	11.5
4	47	30	17

A hysteresis in generated current between heating and cooling steps is evident in Figure 5-9. The reason for the observed hysteresis is due to the difference in thermal gradients across the thermopile during heating and cooling under these transient conditions. The generated current resulted in an efficient charge-up of the battery voltage, shown in Figure 5-10. Over the course of the entire 6-hour experiment, the battery voltage went up from 3.85 V to 3.97 V, an increase of 0.12 V. The results of Wellbore Test 2 show that the injection of heater water results in a generation of a current and storage of power in the on-board battery, constituting a successful demonstration of the tool operation.

When the tool was extracted, the interior of the tool was dry, showing that the leaking fitting had indeed been properly repaired by APS staff.

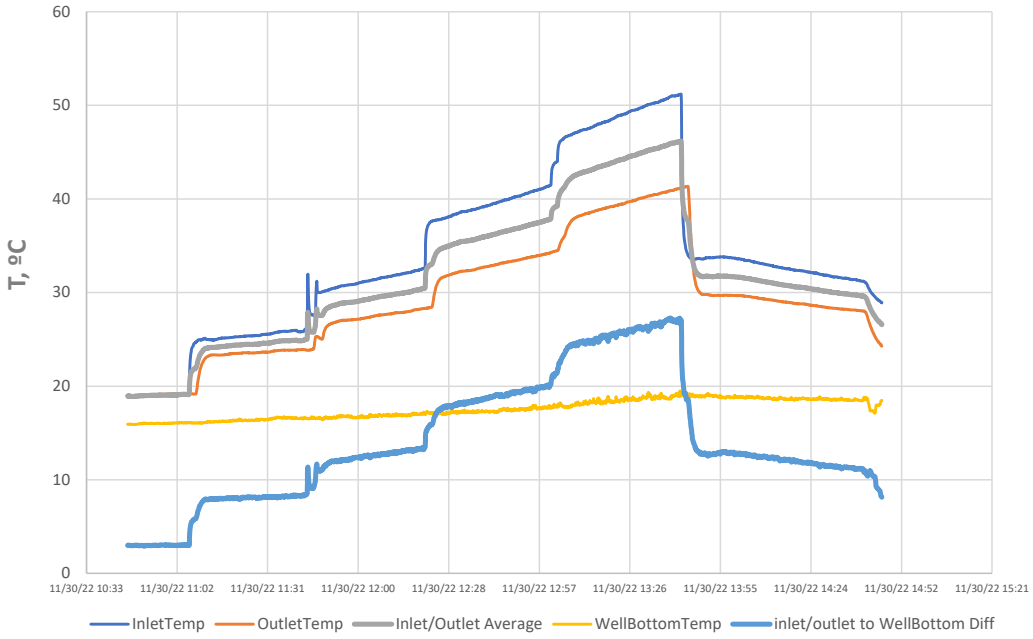

Figure 5-7. External thermocouple response to injection of heated water in four distinct pulses lasting approximately 40 minutes each, followed by a cooldown stage. The light blue line is temperature recorded at the fluid inlet, the light orange line is recorded at the tool outlet, and the yellow line is the temperature of a thermocouple positioned at the tool midpoint but arranged such that it measured water temperature outside of the immersed tool. The gray line is the average of the inlet and outlet temperature, and the thick blue line is the difference between the average and the wellbore water temperature.

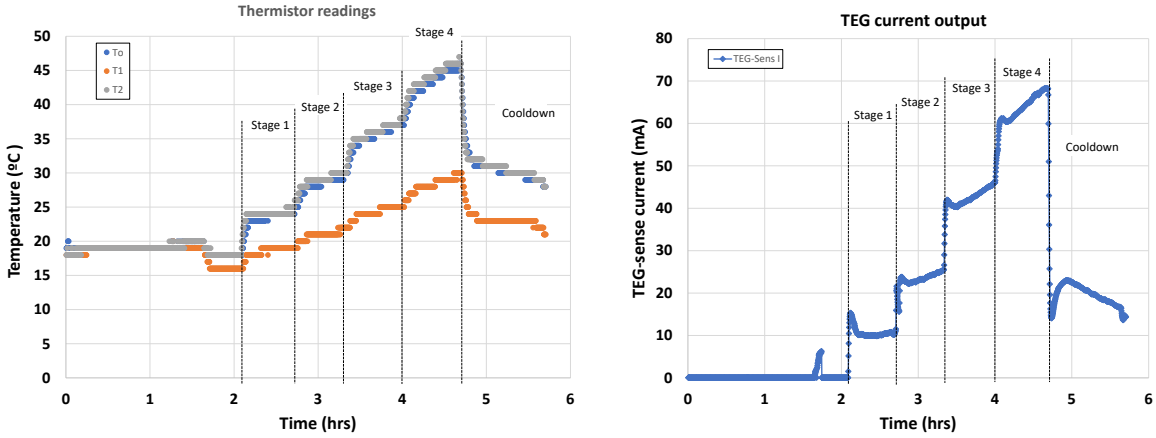

Figure 5-8. Changes in internal thermistor temperatures (T0, T1, and T2) and TEG sense current during Wellbore Test 2. Time 0 is when the tool was sealed, and the next 60 minutes correspond to when the tool was undergoing a helium leak test. The tool encountered the water table at about 90 minutes (with a corresponding drop in temperature) and then heated fluid injection commenced just after 120 minutes. Four stepwise pulses lasting roughly 40 minutes each with stepwise increase in heating result in four steps of increasing current. A fifth cooling step commenced after about 4.7 hours and lasts for approximately 40 minutes, after which the fluid flow was turned off and the tool was extracted from the wellbore.

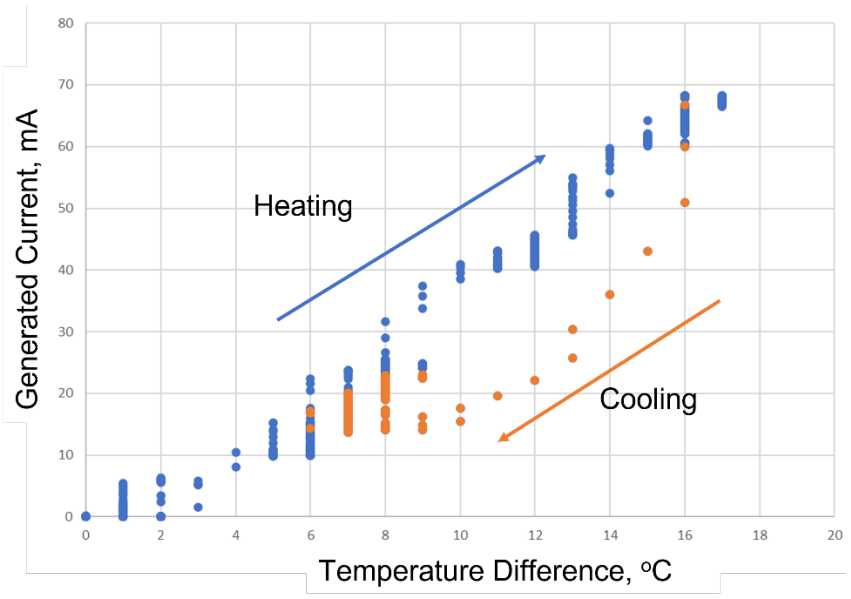

Figure 5-9. Hysteresis in generated current during heating and cooling steps.

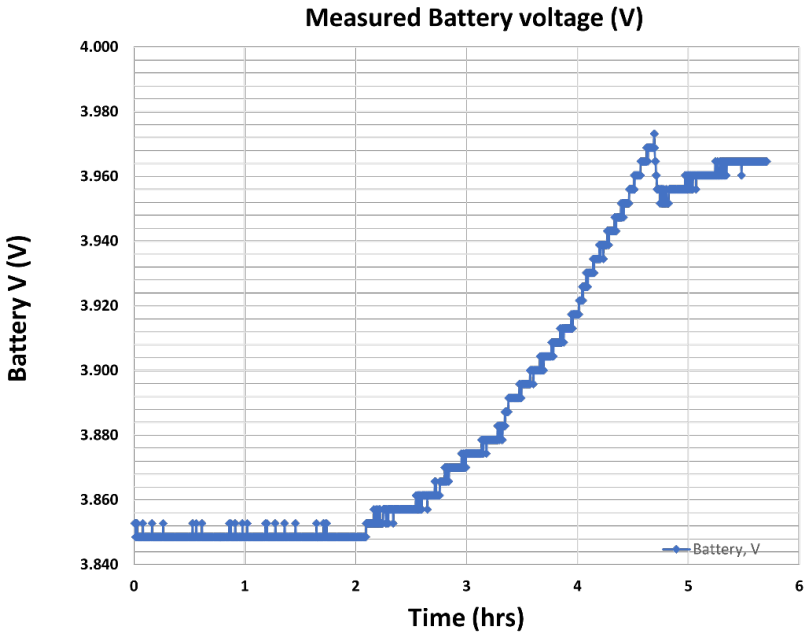

Figure 5-10. Increase in battery voltage during heating of Wellbore Test 2.

5.2.3. Pressure Vessel Test

The third and final test at APS involved testing the operation of the tool at high pressure and temperature conditions, measuring both current generation under conditions approaching those in the subsurface associated with geologic carbon storage, but also testing the resiliency/survivability of the tool at pressure conditions. After the Wellbore Test 2 was successfully carried out, data was wiped from the on-board tool and the data acquisition was initiated, this time at a much slower rate of once per ten minutes. The polarity of the TEG-to-board electronics was switched to allow for a hotter exterior, rather than a hotter interior as occurred during the wellbore tests. The tool was sealed and again subject to a healing leak test, testing the viability of the O-ring seals. APS staff grew concerned that the O-ring clearance in the tool gaps were too large to survive the planned external pressure of 3000 psi (fearing O-ring extrusion and loss of sealing ability), so it was decided that the pressure vessel test would commence with an external pressure of 500 psi, and an internal pressure of 6000 psi (as originally planned, to mimic the effect of fluid injection into the reservoir). Images of the assembled piping to enable the higher internal temperature, and the insertion of the tool inside the APS pressure vessel are shown in Figure 5-11.

Figure 5-11. From left: The TEG tool shown attached to the top closure of the pressure vessel at APS, showing the high-pressure piping used to produce the high internal pressure in the tool; toll and vessel closure hoisted by a crane and inserted into the top of the building used to house the large pressure vessel at APS; top closure at attached tool being lowered into the pressure vessel at APS prior to pressure testing and heating.

During this test, the pressure conditions were first established (Figure 5-12) and then maintained while the vessel was heated. This occurred approximately 24 hours after the tool was sealed, and the heating induced a brief period of generated current due to the difference in the external and internal tool temperatures. After sufficient heating, the internal and external temperatures equilibrated, and current generation ceased. When the instrument was extracted from the pressure vessel, the interior was bone dry with no indication of leaking. This test shows that the TEG tool could survive at high pressure conditions. Sandia and APS staff have discussed how to modify the O-ring sealing structure (involving backer-rings composed of poly-ether-ether-ketone or PEEK) to improve on the original design.

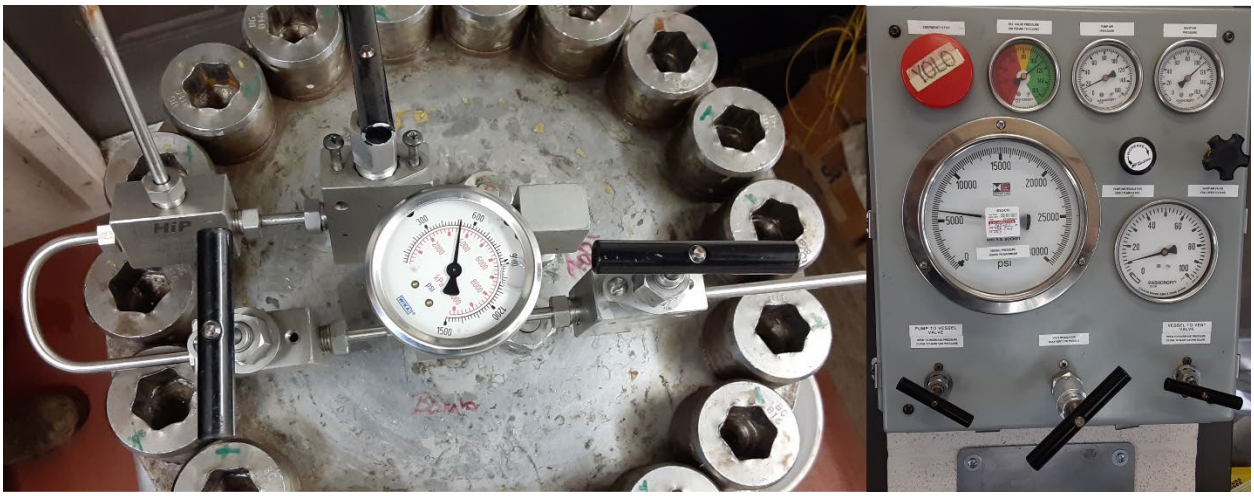

Figure 5-12. Pressure conditions maintained during the pressure vessel test. (Left, external pressure vessel temperature of ~500 psi; Right: internal pressure of ~ 6000 psi (left gauge).

Although the primary purpose of the test was to test tool survivability, temperatures and power generation were monitored during the test as well. These are shown in Figure 5-13. Note that because the heat flux was now from the outside towards the inside, T_0 and T_2 are now the cold side, and T_1 represents the hot side. Because of the time required to set up the experiment, the test was not initiated until almost 30 hours after the tool was sealed and recording was initiated. The test itself lasted only a few hours. The pressure was ramped up to the set values, and then external temperature was rapidly increased by heating the outside of the pressure vessel. This led to a temperature gradient between the outside and inside of the power harvester, with heat flux going into the harvester in this test. For this reason, the leads from the TEGs to the PCB were reversed relative to the earlier downhole test. As the temperature ramped up, the power harvester generated significant power, up to 45 mA at the maximum ΔT. The power generation decreased as the system equilibrated and dropped to zero as the system equilibrated. Power was not generated during the cooling period because the temperature gradient was now reversed with the heat flux out of the instrument.

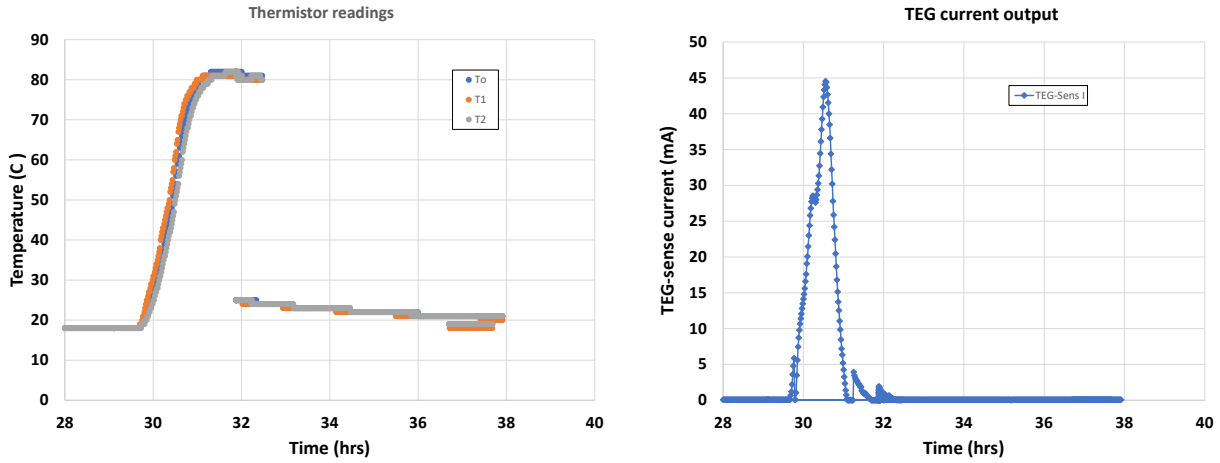

Figure 5-13. Changes in internal thermistor temperatures (T0, T1, and T2) and TEG sense current during the pressure vessel test. Time 0 is when the tool was sealed. Approximately 30 hours after the tool was sealed up, the pressure conditions were induced and stabilized, and then the pressure vessel was heated to approximately 80 ºC. The rise in temperature at about 30 hours induces a rapid increase in generated current. The current decreases back to zero as the tool internal temperature equilibrates with the external vessel temperature, and during the colling period after the heater is cut off.

5.2.4. Summary of the field test results

Once the leaking He test port was repaired, the power generation test went smoothly, and demonstrated that of in situ down-hole power harvesting using thermopile arrays is a feasible approach for wirelessly generating power for subsurface sensor arrays. The amount of power generated by the small field prototype, with only 40 TEGs, is sufficient to fully charge the high temperature battery (500 mAh) using a thermal pulse of a few days, depending upon the thermal gradient produced. However, the design is easily expanded to include more thermopiles, reducing the required duration of the thermal pulse, or to include more batteries to reduce the required frequency of thermal pulses.

Because of the out-of-tolerance machining for the outer shell, the high pressure/high temperature survivability test had to be carried out at a reduced external pressure of 500 psi to mitigate the possibility of O-ring extrusion. However, the tool was designed with a considerable safety margin, and with a properly machined outer shell, should easily be able to survive anticipated borehole pressures. If future testing is done, it is recommended that O-ring backers be used to further mitigate the possibility of O-ring extrusion.

6. Lessons Learned and recommendations for future work.

Lessons learned

The difficulties associated with carrying out a field test provided opportunities for important lessons learned. Specifically, the cost and level of effort required to perform an actual field test in a $scCO_2$ injection well was underestimated. Performing such a test requires pulling and replacing the tubing in a well at least twice; that includes placing packers. This is an expensive undertaking, and in not without risk to the borehole. It proved impossible to carry out such a test, and even at a much higher budget, would have entailed significant risk. Moreover, performing such a test does not allow for error or unanticipated events. For instance, in our tests at the APS Technology Drilling Test Center, the facilities were available to repair the power harvester when a leak occurred, allowing recovery and performance of a successful second test. At an actual $scCO_2$ injection site, such a repair would not have been possible, and the leak would not have been identified until the end of the test and recovery of the tool, days or weeks after emplacement. Repairing and successfully testing the instrument would not have been possible. The APS facility was an ideal location for the actual test. An important lesson learned is that a test of a field prototype at a facility equipped to evaluate borehole technologies is a far better option than moving directly to a field test at a real CO_2 sequestration or EOR site.

Recommendations for future work.

The field prototype produced for this project was intended to demonstrate the feasibility of *in situ* downhole power generation with TEGs. It was not optimized for use as an actual power source for borehole sensors. If the opportunity presents itself for a test in a real $scCO_2$ sequestration borehole some modifications would be required. Specifically, the existing power conditioning board can only charge the battery with a TEG voltage below 2.5 V; above a voltage of 2.5V, the ePeas® power conditioning chip shuts down and does not charge the battery. Using a power conditioning chip with a higher maximum input voltage would improve power generation. Moreover, the board is designed to produce power only when voltage of a single polarization is supplied; hence, power can only be produced during one leg of a thermal pulse. The electronics could be modified to be bidirectional by adding a bridge rectifier, producing power from heat flux in both directions—during both legs (e.g., the ramp-up and cool-down) of a thermal pulse. However, the bridge rectifier results in power loss and voltage drop in the TEG output and is only a viable option if there is sufficient power to spare. Finally, the memory for data storage on the power conditioning board was limited, allowing data collection only over a short test period—a few days maximum. For a longer down-borehole test, additional memory would have to be added to the board. This is readily accomplished.

Potential future funding and future collaborations will also be pursued. This project focused on power generation; integration with subsurface sensors being developed by other projects and with potential data/power transmission approaches being developed to communicate with sensors outside the borehole, is required. Collaboration with those sensor projects will be pursued as opportunities arise. As protection of USDWs is a major objective of the EPA UIC-VI Rule (EPA, 2013), improved real-time, long-term monitoring of external mechanical integrity, that is, fluid movement behind casing, could be a potential application of the thermopile power harvester. The tool could be placed at strategic locations, guided by prior wireline logging, on tubing at depths near the caprock and between the caprock and USDWs to supply power to permanently deployed sensors within or perhaps outside the casing (if communication through casing is developed), such as temperature sensing or acoustic sensors (e.g., potentially pulse-echo or flexural wave) that would

potentially perform better in terms of accuracy and sensitivity than other methods (e.g., distributed fiber sensing).

7. Conclusions.

Robust *in situ* power harvesting underlies all efforts to enable downhole autonomous sensors for real-time and long-term monitoring of CO_2 plume movement and permeance, wellbore health, and induced seismicity. The objective of this project is to evaluate the potential use of downhole thermopile arrays, known as thermoelectric generators (TEGs) as power sources to charge sensors for *in situ* real-time, long-term data capture and transmission. Real-time downhole monitoring will enable "Big Data" techniques and machine learning, using massive amounts of continuous data from embedded sensors, to quantify short- and long-term stability and safety of enhanced oil recovery and/or commercial-scale CO_2 storage.

In this project, we evaluated possible placement of the TEGs at two different wellbore locations, on the outside of the casing, or on the production tubing. TEGs convert heat flux to electrical power, and in the borehole environment, would convert heat flux into or out of the borehole into power for downhole sensors. Such heat flux would be driven by pumping of fluids into or out of the borehole—for instance, injecting supercritical CO_2—creating a thermal pulse that could power the downhole sensors. Hence, wireless power generation could be accomplished with *in situ* TEG energy harvesting.

This project final report provides a summary of the thermopile project. It provides background and summarizes the work done for the project, including selection of materials, fabrication of a laboratory benchtop prototype, and experiments and thermal-hydrologic modeling carried out to design and optimize a field-scale power generation test unit. Finally, it describes the prototype field unit that has been built and presents the results of field tests carried out with the field prototype. The field tests evaluated both downhole power generation in response to a thermal gradient produced by pumping a heated fluid down a borehole, and component survivability and operation at elevated temperatures and pressures. The field tests demonstrated the feasibility of the TEG energy harvesting approach for borehole applications. One potential use is generating power and acting as a data hub for long term storage of data for downhole sensors. Theses could be co-located sensors wired to the power harvester within a borehole, or could be external to the borehole, if technologies that are currently under study to transmit power and data through the borehole casing can be perfected.

Another perspective on this project's accomplishments is from that of Technical Readiness Levels (TRLs) and intellectual property protection to accelerate deployment of robust downhole tools for monitoring commercial scale CO_2 storage sites. This project traversed TRL-1 through TRL-5 by the following: first developing basic concepts for the tool, including formulation of the application with input from actual downhole CO_2-enhanced oil recovery field conditions (e.g., from the SWP) including wellbore and tubing sizes, and downhole pressure and temperature during CO^2-enhanced oil recovery operations; modeling and preliminary prototype lab testing to support designs of a full-scale field unit; and performance and survivability testing to verify operation of the fully assembled field unit in relevant environments with thermal pulses via fluid flow in a shallow borehole for power generation, and confirmation of proper functioning at reservoir relevant pressure (external pressure of ~500 psi or 3.45 MPa and internal pressure of ~6,000 psi or 41.4 MPa) and temperature (up to ~80°C). Future work with deployment on tubing to the depths of underground sources of drinking (USDWs) and confining units, with connection to sensors or other instrumentation, would move the technology to TRL-6 or higher. A fully-issued patent has been accepted for the thermopile concept for downhole monitoring applications (Bryan et al., 2022), which will support future technology transfer to industry. TRL concepts used here are adapted from NASA (2023), and

USDOE (2019), as the authors of this current report have not found an Office of Fossil Energy and Carbon Management-specific guide for TRLs and technology development.

8. References

Bryan, C.R., Heath, J.,E., Koripella, C.R., Dewers, T. 2022. System and method thermopile energy harvesting for subsurface well bore sensors. United States Patent, Patent No.: US 11,319,779 B1. Date of Patent: May 3, 2022.

Heath, J., Dewers, T., Cather, M. 2021. Core Analysis E-Reports Produced for the Southwest Regional Partnership on Carbon Sequestration for Wells 13-10A, 13-14, and 32-8 of the Farnsworth Unit, Texas, 6/23/2021, https://edx.netl.doe.gov/dataset/core-analysis-e-reports-for-the-swp, doi: 10.18141/1798503.

Hurter, S., Garnett, A., Bielinski, A., Kopp., A. 2007. Thermal signature of free-phase CO_2 in porous rocks: detectability of CO_2 by temperature logging. Society of Petroleum Engineers, SPE 109007, Offshore Europe 2007.

Moodie, N., Ampomah, W., Heath, J., Jia, W., and McPherson, B. 2021. Quantitative analysis of the influence of capillary pressure on geologic carbon storage forecasts case study: CO2-EOR in the Anadarko basin, Texas. International Journal of Greenhouse Gas Control 109, https://doi.org/10.1016/j.ijggc.2021.103373.

National Aeronautics and Space Administration (NASA), 2023, Technology Readiness Level Definitions, https://www.nasa.gov/pdf/458490main_TRL_Definitions.pdf, retrieved 1/16/23.

National Energy Technology Laboratory (NETL). 2021. Carbon Storage Program. https://netl.doe.gov/sites/default/files/2022-08/Program-116.pdf, retrieved 1/17/23.

Rhino, K., Iyer, J., Walsh, S.D.C., Carroll, S.A., Smith, M.M. 2021. Influence of effective stress and transport on mechanical alteration processes at the Cement-Caprock interface. International Journal of Greenhouse Gas Control 109, 103340, https://doi.org/10.1016/j.ijggc.2021.103340.

Simmons, J., Rinehart, A., Luhmann, A., Mozley, P., Heath, J., Majumdar, B. 2022. Using petrographically observable microstructure to predict hydromechanical changes in a complex siliciclastic storage site during CO_2 injection. International Journal of Greenhouse Gas Control 119, 103724, https://doi.org/10.1016/j.ijggc.2022.103724.

Trujillo, N., Rose-Coss, D., Heath, J.E., Dewers, T.A., Ampomah, W., Mozley, P.S., and Cather, M. 2021. Multiscale assessment of caprock integrity for geologic carbon storage in the Pennsylvanian Farnsworth Unit, Texas, USA. Energies 2021, 14(18), 5824, https://doi.org/10.3390/en14185824.

Xiao, T., McPherson, B., Bordelon, A., Viswanathan, H., Dai, Z., Tian, H., Esser, R., Jia, W., Carey, B. 2017. CO_2-cement-rock interactions at the well-caprock-reservoir interface and implications for geological CO_2 storage. International Journal of Greenhouse Gas Control 63, 126–140, https://doi.org/10.1016/j.ijggc.2017.05.009.

United States Department of Energy (DOE). 2017. Report of the Mission Innovation Carbon Capture, Utilization, and Storage Experts' Workshop. Mission Innovation, DOE, https://www.energy.gov/fecm/downloads/accelerating-breakthrough-innovation-carbon-capture-utilization-and-storage, retrieved 1/17/23.

United States Department of Energy (USDOE), 2019, Appendix F – Technical Readiness Assessment Methodology, in: Report on the Status of the Solid Oxide Fuel Cell Program. United States Department of Energy, Washington, DC, https://www.energy.gov/fe/downloads/appendix-f-trl-guide, retrieved 1/16/23.

United States Department of Energy (DOE). 2020. Office of Clean Coal and Carbon Management Strategic Vision 2020-2024. Office of Fossil energy, https://www.energy.gov/sites/prod/files/2020/08/f77/FE-20%20Strategic%20Vision%20FINAL%202020_Aug_12_compliant.pdf, retrieved 1/17/23.

United Sates Environmental Protection Agency (EPA). 2013. Geologic Sequestration of Carbon Dioxide Underground Injection Cntrol (UIc) Program Class VI Well Testing and Monitoring Guidance. Office of Water (4606M), EPA 816-R-13-001, https://www.epa.gov/sites/default/files/2015-07/documents/epa816r13001.pdf, retrieved 1/17/23.

Wu, Z., Luhmann, A.J., Rinehart, A.J., Mozley, P.S., Dewers, T.A., Heath, J.E., Majumdar, B.S. 2020. Chemo-mechanical alterations induced from CO2 injection in carbonate-cemented sandstone: an experimental study at 71 degrees C and 29 MPa. Journal of Geophysical Research-Solid Earth 125(3), e2019JB019096, https://doi.org/10.1029/2019JB019096.